arXiv:1403.7137v1 [cs.CE] 27 Mar 2014

Computer Science Technical Report
CSTR-4/2014
March 28, 2014

Ahmed Attia and Adrian Sandu

"A Sampling Filter for Non-Gaussian Data Assimilation"

Computational Science Laboratory
Computer Science Department
Virginia Polytechnic Institute and State University
Blacksburg, VA 24060
Phone: (540)-231-2193
Fax: (540)-231-6075
Email: sandu@cs.vt.edu
Web: http://csl.cs.vt.edu

Innovative Computational Solutions

A Sampling Filter for Non-Gaussian Data Assimilation

Ahmed Attia[a], Adrian Sandu[a,*]

[a] *Computational Science Laboratory*
Department of Computer Science
Virginia Polytechnic Institute and State University
2201 Knowledgeworks II, 2202 Kraft Drive, Blacksburg, VA 24060, USA
Phone: 540-231-2193, Fax: 540-231-9218
E-mail: sandu@cs.vt.edu

Abstract

Data Assimilation in operational models like atmospheric or Ocean models is almost impossible without posing many assumptions due to the complication of the model that is usually very high-dimensional and also due to non-linearity of the observation operator used to map the state space to the measurement space. Ensemble Kalman filter (EnKF) is the most popular ensemble-based data assimilation approach due its simple formulation, ease of implementation, and satisfactory results. All variants of EnKF assume that the posterior (analysis PDF) distribution is Gaussian and they tend to fail when nonlinear observation operators are incorporated. Although the Gaussian assumption is widely accepted, however, it turns out to be too restrictive. Several techniques have been proposed to deal with non-linearity in measurements, for example the maximum likelihood ensemble filter (MLEF) is one of the most successful strategies but it has its own downsides. MLEF estimates the analysis state of the system as the maximum a posteriori estimate (MAP) assuming the posterior distribution is Gaussian, and it is designed to work with nonlinear and even non-differentiable observation operators. MLEF shows satisfactory performance with weekly nonlinear observation operators, however it fails in many instances where high-dimensionality and/or strong non-linearity take place. In this paper, we propose a new ensemble-based data assimilation method, named "*sampling filter*". The filter is used to sample directly from the posterior distribution. The sampling strategy in the analysis phase of the filter follows a Hybrid Monte Carlo (HMC) approach that is, in principle, applicable in cases where Gaussian assumption is violated. In this work, the posterior is assumed to be Gaussian as a first step but we used several observation operators with different levels of non-linearity and differentiability. Several experiments testing the potential and performance of the proposed algorithm and comparing its performance with both EnKF and MLEF using six different observation operators are conducted. The Lorenz-96 model is used and the results are compared to EnKF and MLEF. The results show that this approach is promising, mostly with the new developments proposed recently in HMC sampling literature.

Keywords: Data Assimilation, Variational Methods, Ensemble Filters, Hybrid Methods

Contents

1 Introduction **3**

2 Data Assimilation **4**
2.1 DA: problem statement 4
2.2 Ensemble-based DA: EnKF 5
2.3 Ensemble-based DA: MLEF 7

3 Markov Chain Monte Carlo Sampling and the Hybrid MCMC **9**
3.1 HMCMC sampling 9
3.2 Hamiltonian equations 10
3.2.1 Position Verlet Integrator 11
3.2.2 Two-stage integrator 12
3.2.3 Three-stage integrator 12
3.2.4 Four-stage integrator 13
3.2.5 General integrator defined on Hilbert space 13
3.3 HMCMC sampling algorithm 13

4 Sampling Filter **15**
4.1 Sampling filter algorithm 16

5 Experiment Design **17**
5.1 Lorenz-96 model 17
5.2 Observations and observation operators 17
5.2.1 Linear observation operator 17
5.2.2 Quadratic observation operator 17
5.2.3 Cubic observation operator 18
5.2.4 Magnitude observation operator 18
5.2.5 Quadratic observation operator with a threshold 18
5.2.6 Exponential observation operator 18

6 Results **18**
6.1 Linear observation operator experiments 19
6.2 Quadratic observation operator experiments 22
6.3 Cubic observation operator experiments 24
6.4 Absolute value observation operator experiments 27
6.5 Quadratic observation operator (with a threshold) experiments 29
6.6 Exponential observation operator (with factor $r = 0.2$) experiments 32
6.7 Number of steps in MC between successive state selections 34
6.8 Adding more difficulty 37

*Corresponding author

7 Conclusion and Future Work **40**

1. Introduction

Unlike Variational methods, ensemble-based data assimilation techniques do not require derivation of a tangent linear operator or adjoint equations [1] or even backward integration in time as in 4DVAR method for example. The ensemble Kalman Filter introduced by Evensen [2] is currently the most popular ensemble-based sequential data assimilation scheme. Many variants of the basic formulation of EnKF are available. EnKF formulations fall in one of two classes, namely, stochastic and deterministic formulations [3]. In the stochastic approach, each ensemble member is updated using a perturbed version of the observation vector to prevent ensemble collapse [4, 5]. On the other hand, in deterministic formulation (also known as Square Root Ensemble Filters,) the observations are used to assimilate each ensemble member without adding any noise.

All variants of the EnKF compete in performance and accuracy in case of linear observations, however, realistic observation operators are generally nonlinear. EnKF equations, in case of nonlinear observation operators, are derived using linearized version of the model and the observation operator starting with the Extended Kalman filter (EKF) equations [6]. There are also two common approaches to handle non-linearity of observations instead of using the linearized observation operator; The first strategy is to use the difference between two nonlinear operators instead of the linearized version assuming first order Taylor series approximation. This approache usually results in mathematical inconsistency in handling the nonlinear operators [6]. Another approach is to pose a nonlinear problem at first, then search for the best solution in a subspace spanned by the ensemble members. The maximum likelihood ensemble filter (MLEF) follows the latter strategy to deal with nonlinear observation operators.

MLEF presented by Zupanski [6] finds an analysis solution that maximizes the likelihood of the posterior probability distribution (posterior PDF), through a minimization process of a cost function that depends generally on a nonlinear observation operator. This scheme has a main advantage, that it doesn't require the observation operator to be differentiable and does not use finite difference approximation of the tangent model of the observation operator (e.g. the Jacobian). However, this approach tends to diverge if the observation operator is highly nonlinear. Also it is inherently assumed that the posterior distribution is Gaussian and hence the maximum a posteriori probability estimate is meaningful and useful. Unfortunately, in case of multimodal distributions this technique tends also to fail.

A perfect ensemble-based data assimilation filtering technique that is operational and successful in case of non-Gaussian posterior and nonlinear observations is yet to be found.

The current advance in sampling algorithms makes it compulsory to think of direct sampling from the posterior probability distribution of the system state. Markov Chain Monte Carlo (MCMC) is a Monte Carlo sampling strategy that works by generating a Markov chain whose invariant (stationary) distribution is the target PDF that is to be sampled from.

Monte Carlo sampling techniques in general, are theoretically useful and result in representative samples in case of low-to-moderate dimensional distributions. However, they occasionally fail in case of large dimensions where very complicated PDFs are to be sampled from. Hybrid Markov Chain Monte Carlo (HMCMC) algorithm is a variant from MCMC sampling that incorporates a potential variable from a Hamiltonian system as auxiliary variable. This sampling scheme turns out to be very useful in sampling from complicated and high dimensional distribution.

In this paper, we describe a fully nonlinear filtering technique that uses a HMCMC sampling strategy to sample from the posterior PDF based on linear or nonlinear observation operators. The proposed filter doesn't require the target probability distribution to be Gaussian, however, we assume it is Gaussian as a first step and also to compare it with both EnKF and MLEF. Non-Gaussian assumption will be tested in future work with applications of the sampling filter to a high-resolution operational models.

The paper is organized as follows: an overview of data assimilation and the widely-used solution strategies is given in Section 2, MCMC and HMC background and algorithms are summarized in Section 3, the sampling filter details will be given in Section 4, experimental design presented in Section 5, results in Section 6, and conclusions with future work given in Section 7.

2. Data Assimilation

This section is devoted to providing a brief overview of the general statement and the current solution strategies of the Data Assimilation (DA) problem. In addition, it also highlights the motivation behind our research presented in this paper.

2.1. DA: problem statement

Consider a forward model that propagates the initial model state (initial condition) $\mathbf{x}_0 = \mathbf{x}(t_0) \in \mathbb{R}^{\mathrm{N_{var}}}$ to a future state $\mathbf{x}_k = \mathbf{x}(t_k) \in \mathbb{R}^{\mathrm{N_{var}}}$, that is:

$$\mathbf{x}_k = \mathcal{M}_{t_0 \to t_k}(\mathbf{x}_0) \ , \quad t_0 \leq t_k \leq t_F \, , \tag{1}$$

where t_0 and t_F are the beginning and the end points of the simulation time interval.

The model solution operator $\mathcal{M}$ represents, for example, a discrete approximation of the partial differential equations that govern the evolution of the dynamical system (e.g. atmospheric or oceanic processes). Realistic atmospheric and ocean models typically have $\mathrm{N_{var}} \sim 10^6 - 10^9$ variables.

While the forward model $\mathcal{M}$ is used to propagate the state of the system to future times, perturbations (small errors $\delta\mathbf{x}$) of the state of the system maybe simultaneously evolved according to the linearized model operator $\mathbf{M} = \mathcal{M}'$, which is called the tangent linear model:

$$\delta\mathbf{x}_k = \delta\mathbf{x}(t_k) = \mathbf{M}_{t_0 \to t_k}(\mathbf{x}_0) \cdot \delta\mathbf{x}_0 \ , \quad t_0 \leq t_k \leq t_F. \tag{2}$$

Usually, the initial model state is uncertain and a better state estimate is sought of based on any available measurements. The model (1) simulation from time t_0 to t_F is initialized

with the background (prior estimate) $\mathbf{x}_0^{\mathrm{b}} = \mathbf{x}^{\mathrm{b}}(t_0)$ of the true state $\mathbf{x}_0^{\mathrm{true}} = \mathbf{x}^{\mathrm{true}}(t_0)$ (atmosphere state for example) that is to be estimated as accurate as possible. The background represents the best estimate of the true state *prior* to any measurement being available. The background errors (uncertainties) are generally assumed to have a Gaussian distribution, that is $\mathbf{x}_0^{\mathrm{b}} - \mathbf{x}_0^{\mathrm{true}} \in \mathcal{N}(0, \mathbf{B}_0)$, where $\mathbf{B}_0$ is the background error covariance matrix. This assumption is a widely accepted assumption and we will follow it.

Observations of the true state $\mathbf{y}_k = \mathbf{y}(t_k) = \mathcal{H}_k(\mathbf{x}_k) + \varepsilon_k$ are available at each time instant $t_k,\ k = 0, 1, \ldots, \mathrm{N_{obs}} - 1$, such that $t_0 \leq t_k \leq t_F\ \forall\ k = 0, 1, \ldots, \mathrm{N_{obs}} - 1$. Here $\mathrm{N_{obs}}$ refers to the number of observation time points in this simulation interval (assimilation window). The observation operator $\mathcal{H}_k$ maps the state space to the observation space at time t_k. These observations are corrupted by measurement and representativeness errors [7], which are also assumed to have a normal distribution, $\varepsilon_k \in \mathcal{N}(0, \mathbf{R}_k)$, where $\mathbf{R}_k$ is the observation error covariance matrix at time t_k. Data assimilation combines the background estimate $\mathbf{x}_0^{\mathrm{b}}$, the measurements $\mathbf{y}_0, \mathbf{y}_1, \ldots, \mathbf{y}_{\mathrm{N_{obs}}-1}$, and the model $\mathcal{M}$ to obtain an improved estimate $\mathbf{x}_0^{\mathrm{a}}$ of the true initial state $\mathbf{x}_0^{\mathrm{true}}$. This improved estimate $\mathbf{x}^{\mathrm{a}}$ is called the "*analysis*" (or *posterior* estimate) of the state of the system. Note that in the simplest case we may have $t_F = t_0$ and observation vector is available only at that time point which leads to the sequential form of data assimilation.

There are currently two main approaches for solving the data assimilation problem, variational methods and ensemble-based methods. The sampling filter proposed in this paper belongs to the ensemble-based solutions. The two ensemble filters, EnKF and MLEF, are reviewed in what follows.

2.2. Ensemble-based DA: EnKF

Kalman filters (KF) [8, 9] in general are viewed as sequential data assimilation methodologies, which means that the state of the system is propagated forward in time by the full model and whenever measurements are available, they are assimilated to the state of the system, and the model is reinitialized to the produced analysis and the process continues.

The sequential data assimilation algorithms proceed in two main steps, namely, *forecast* and *analysis* steps. In the forecast step, the state of the system is propagated forward by the model equations (1) to the next time point where observations are available, producing a forecast of the state of the system, and a forecast error covariance matrix is presented to quantify the uncertainty of the forecast. The forecast state is:

$$\mathbf{x}_k^{\mathrm{f}} = \mathcal{M}_{t_{k-1} \to t_k}(\mathbf{x}_{k-1}^{\mathrm{a}}). \tag{3}$$

A typical assumption is that while the state evolves according to nonlinear dynamics (1), small errors evolve according to the linearized model (2). If the errors in the model state at time t_{k-1} have a normal distribution $\mathcal{N}(0, \mathbf{A}_{k-1})$ and propagate according to the linearized modes dynamics (2), then the forecast errors at t_k are also normally distributed $\mathcal{N}(0, \mathbf{A}_k)$. The forecast error covariance matrix is then obtained using:

$$\mathbf{B}_k = \mathbf{M}_{t_{k-1} \to t_k} \mathbf{A}_{k-1} \mathbf{M}_{t_{k-1} \to t_k}^T + \mathbf{Q}_{k-1}\,, \tag{4}$$

where $\mathbf{M}^T_{t_{k-1}\to t_k}$ is the adjoint of the tangent linear model, and $\mathbf{Q}_{k-1}$ is the covariance matrix of cumulative model errors between time t_{k-1} and time t_k [10, 11]. In this paper we will consider perfect models, i.e., we will assume $\mathbf{Q} = 0$ for now on.

The analysis step provides the assimilated (improved) estimate of the state $\mathbf{x}^{\mathrm{a}}_k$ and the corresponding error covariance matrix $\mathbf{A}_k$ to quantify the uncertainty in the analysis [12]

$$\mathbf{x}^{\mathrm{a}}_k = \mathbf{x}^{\mathrm{f}}_k + \mathbf{K}_k(\mathbf{y}_k - \mathbf{H}_k\mathbf{x}^{\mathrm{f}}_k)\,, \tag{5a}$$

$$\mathbf{A}_k = \mathbf{B}_k - \mathbf{K}_k\mathbf{H}_k\mathbf{B}_k\,, \tag{5b}$$

$$\mathbf{K}_k = \mathbf{B}_k\mathbf{H}_k^T(\mathbf{H}_k\mathbf{B}_k\mathbf{H}_k^T + \mathbf{R}_k)^{-1}\,, \tag{5c}$$

where $\mathbf{K}_k$ is the Kalman gain. The observation operator is assumed to be linear, that is $\mathcal{H}(\mathbf{x}_k) = \mathbf{H}_k\mathbf{x}_k$ which guarantees the optimality of the solution obtained by the Kalman filter. There are formulations that use a linearized version (e.g. the Jacobian) of the observation operator, however, all are suboptimal and fail at some point, and this is the main motivation of our research as we will show later in more details.

The storage and computational requirements of the forecast and analysis error covariance matrices make the basic formulation of Kalman filter non-practical. The ensemble Kalman filter (EnKF) is an ensemble-based version of the Kalman filter, that uses an ensemble of states to represent the state space of the discretized version of the system. Many variants exist in the literature, however they all follow the same strategy. In EnKF, a full ensemble of states is propagated forward in time, and all are assimilated by the observation vector (or perturbed versions of it).

There are two main approaches for the assimilation step; deterministic and stochastic methods and they mainly differ in the way the observation vector is assimilated to the forecast ensemble of states resulting in the analysis ensemble of states [3]. The stochastic ("*perturbed observations*") version [4] of the ensemble Kalman filter uses a Monte-Carlo approach to propagate covariances while treating the observations as random variables. An ensemble of $\mathrm{N_{ens}}$ states (labeled $e = 1, \ldots, \mathrm{N_{ens}}$) is used to sample the probability distribution of the background error. Each member of the ensemble (with state $\mathbf{x}^{\mathrm{a}}_{k-1}(e)$ at t_{k-1}) is propagated to t_k using the nonlinear model (1) to obtain the "forecast" ensemble $\mathbf{x}^{\mathrm{f}}_k(e)$. If the model errors are considered, Gaussian noise $\eta_k \in \mathcal{N}(0, \mathbf{Q}_k)$ is added to the forecast to account for the effect of model errors. The mean of the analysis ensemble ($\overline{\mathbf{x}}^{\mathrm{a}}_k$) is used as the analysis estimate of the state of the system. The forecast step of the EnKF is governed by the equations [13, 14]:

$$\mathbf{x}^{\mathrm{f}}_k(e) = \mathcal{M}_{t_{k-1}\to t_k}(\mathbf{x}^{\mathrm{a}}_{k-1}(e)) + \eta_k(e), \quad e = 1, \ldots, \mathrm{N_{ens}}\,, \tag{6a}$$

$$\overline{\mathbf{x}}^{\mathrm{f}}_k = \frac{1}{\mathrm{N_{ens}}}\sum_{e=1}^{\mathrm{N_{ens}}}\mathbf{x}^{\mathrm{f}}_k(e)\,, \tag{6b}$$

$$\mathbf{X}^{\mathrm{f}}_k = [\mathbf{x}^{\mathrm{f}}_k(1) - \overline{\mathbf{x}}^{\mathrm{f}}_k, \ldots, \mathbf{x}^{\mathrm{f}}_k(\mathrm{N_{ens}}) - \overline{\mathbf{x}}^{\mathrm{f}}_k]\,, \tag{6c}$$

$$\mathbf{B}_k = \left(\frac{1}{\mathrm{N_{ens}} - 1}\left(\mathbf{X}^{\mathrm{f}}_k\left(\mathbf{X}^{\mathrm{f}}_k\right)^T\right)\right) \circ \rho\,, \tag{6d}$$

where $\overline{\mathbf{x}}^{\mathrm{f}}_k$ is considered the background estimate of the system before assimilation, and ρ is

a localization matrix (generally, a correlation function with local support). Since we assume a perfect model, the model error term $\eta_k(e)$ in equation (6a) vanishes.

Each member of the forecast (ensemble of forecast states) is analyzed separately using the state equations (5). Observation noise $\zeta_k \in \mathcal{N}(0, \mathbf{R}_k)$ is added to each observation, resulting in the following assimilation equations:

$$\mathbf{x}_k^{\mathrm{a}}(e) = \mathbf{x}_k^{\mathrm{f}}(e) + \mathbf{K}_k \left([\mathbf{y}_k + \zeta_k] - \mathbf{H}_k \mathbf{x}_k^{\mathrm{f}}(e) \right), \quad e = 1, \ldots, \mathrm{N_{ens}}, \tag{7a}$$

$$\mathbf{K}_k = \mathbf{B}_k \mathbf{H}_k^T \left(\mathbf{H}_k \mathbf{B}_k \mathbf{H}_k^T + \mathbf{R}_k \right)^{-1}. \tag{7b}$$

The forecast and the analysis error covariances are estimated from the statistical samples ($\{\mathbf{x}_k^{\mathrm{f}}(e)\}_{e=1,\ldots,\mathrm{N_{ens}}}$ and $\{\mathbf{x}_k^{\mathrm{a}}(e)\}_{e=1,\ldots,\mathrm{N_{ens}}}$ respectively).

Square root versions (deterministic formulations) of EnKF avoid explicit construction of the covariance matrices by updating a perturbation matrix only (almost the square root of the covariance matrix).

The main shortcomings of the ensemble Kalman filter are the assumptions of the Gaussianity of the posterior PDF of the analysis states, and the linearity requirement of the observation operator to give useful results.

A linearized version of the EnKF equations is easily formulated (e.g. start with the Extended Kalman filter (EKF) equations) using the Jacobian of the observation operator, $\mathbf{H}_k$, resulting in a linearized ensemble Kalman filter set of equations. However, as we will see in the results, this formulation tends to fail in case of high non-linearity of the observation operator.

2.3. Ensemble-based DA: MLEF

The Maximum Likelihood Ensemble filter (MLEF) is an ensemble-based filtering technique that runs an optimization algorithm (e.g non-linear conjugate gradient or quasi-newton) to obtain an estimate of the analysis state, assuming Gaussian posterior PDF, by minimizing an arbitrary nonlinear objective function [15, 6] on the form:

$$\mathcal{J}(\mathbf{x}) = \frac{1}{2}(\mathbf{x} - \mathbf{x}^{\mathrm{b}})^T \mathbf{B}^{-1} (\mathbf{x} - \mathbf{x}^{\mathrm{b}}) + \frac{1}{2}(\mathbf{y} - \mathcal{H}(\mathbf{x}))^T \mathbf{R}^{-1} (y - \mathcal{H}(\mathbf{x})), \tag{8}$$

and then updating the analysis error covariance matrix based on the fact that it is equal to the inverse of the Hessian matrix at the minimum [16].

Given an initial ensemble of states $\{\mathbf{x}_0(e)\}_{e=1,2,\ldots,\mathrm{N_{ens}}}$, at time t_0 , the MLEF algorithms defines:

$$\mathbf{x}_k^{\mathrm{opt}} = \frac{1}{\mathrm{N_{ens}}} \sum_{e=1}^{\mathrm{N_{ens}}} \mathbf{x}_k(e), \tag{9a}$$

$$\left(\mathbf{A}_k^{\frac{1}{2}} \right)_e = \frac{1}{\sqrt{\mathrm{N_{ens}} - 1}} \left(\mathbf{x}_k(e) - \mathbf{x}_k^{\mathrm{opt}} \right) = \mathbf{a}_{\mathrm{k}}(e), \tag{9b}$$

where $\mathbf{A}_k = \mathbf{A}_k^{\frac{1}{2}} \left(\mathbf{A}_k^{\frac{1}{2}} \right)^T$ is the analysis error covariance matrix, and $\mathbf{a}_{\mathrm{k}}(e)$ is the e^{th} column of the matrix $\mathbf{A}_k^{\frac{1}{2}}$, for each $e = 1, 2, \ldots, \mathrm{N_{ens}}$.

The forecast step is conducted on the optimal solution $\mathbf{x}_{\mathrm{k-1}}^{\mathrm{opt}}$, to get the forecast state at the next time point t_k. A perturbed version of the state is also propagated using the full model as follows:

$$\begin{aligned}
\mathbf{x}_k^{\mathrm{b}} &= \mathcal{M}_{t_{k-1}\rightarrow t_k}(\mathbf{x}_{\mathrm{k-1}}^{\mathrm{opt}})\,, && \text{(10a)}\\
\mathbf{b}_{\mathrm{k}}(e) &= \mathcal{M}_{t_{k-1}\rightarrow t_k}(\mathbf{x}_{\mathrm{k-1}}^{\mathrm{opt}} + \mathbf{a}_{\mathrm{k-1}}(e)) - \mathcal{M}_{t_{k-1}\rightarrow t_k}(\mathbf{x}_{\mathrm{k-1}}^{\mathrm{opt}});\ e = 1, 2, \ldots, \mathrm{N_{ens}}\,, && \text{(10b)}\\
\mathbf{B}_k^{\frac{1}{2}} &= [\mathbf{b}_{\mathrm{k}}(1),\ \mathbf{b}_{\mathrm{k}}(2),\ , \ldots, \mathbf{b}_{\mathrm{k}}(\mathrm{N_{ens}})] \times \alpha\,, && \text{(10c)}
\end{aligned}$$

where α is an inflation factor (slightly more than one) to prevent one of the main drawbacks of the ensemble-based filters widely known as inbreeding [5].

The analysis step starts by presenting the following notations:

$$\begin{aligned}
\mathbf{Z} &= [\mathbf{z}(1),\ \mathbf{z}(2),\ \ldots,\ \mathbf{z}(\mathrm{N_{ens}})]\ , && \text{(11a)}\\
\mathbf{z}(e) &= \mathbf{R}_k^{-\frac{1}{2}}\mathcal{H}_k(\mathbf{x}_k^{\mathrm{b}} + \mathbf{b}_{\mathrm{k}}(e) - \mathbf{R}_k^{\frac{1}{2}}(\mathbf{x}^{\mathrm{b}})\ \forall\ e = 1, 2, \ldots, \mathrm{N_{ens}}\,,\\
&= \mathbf{R}_k^{-\frac{1}{2}}\left(\mathbf{y}_k - \mathcal{H}_k(\mathbf{x}_k^{\mathrm{b}})\right) - \mathbf{R}_k^{-\frac{1}{2}}\left(\mathbf{y}_k - \mathcal{H}_k\left(\mathbf{x}_k^{\mathrm{b}} + \mathbf{b}_{\mathrm{k}}\left(e\right)\right)\right)\ , && \text{(11b)}\\
\mathbf{C} &= \mathbf{Z}^T\mathbf{Z}\,, && \text{(11c)}\\
\mathbf{T} &= (\mathbf{I} + \mathbf{C})^{-\frac{1}{2}};\ \ \mathbf{C} = \mathbf{V}\mathbf{D}\mathbf{V}^T\ \text{(Eigen Decomposition)}\,, && \text{(11d)}\\
&= \mathbf{V}\left(\mathbf{I} + \mathbf{D}\right)^{-\frac{1}{2}}\mathbf{V}^T. && \text{(11e)}
\end{aligned}$$

Next, the optimal solution (mode of the Gaussian posterior PDF) is found by minimizing the following cost function (in the ensemble subspace):

$$\begin{aligned}
\mathcal{J}(\xi) &= \frac{1}{2}\xi^T(\mathbf{I} + \mathbf{C})^{-1}\xi && \text{(12)}\\
&+ \frac{1}{2}\left(\mathbf{y}_k - \mathcal{H}_k\left(\mathbf{x}_k^{\mathrm{b}} + \mathbf{B}_k^{\frac{1}{2}}(\mathbf{I} + \mathbf{C})^{-\frac{1}{2}}\right)\xi\right)^T\mathbf{R}_k^{-1}\left(\mathbf{y}_k - \mathcal{H}_k\left(\mathbf{x}_k^{\mathrm{b}} + \mathbf{B}_k^{\frac{1}{2}}(\mathbf{I} + \mathbf{C})^{-\frac{1}{2}}\right)\xi\right).
\end{aligned}$$

The gradient reads:

$$\nabla_\xi\mathcal{J}(\xi) = (\mathbf{I} + \mathbf{C})^{-1}\xi - \mathbf{T}\mathbf{Z}^T\mathbf{R}_k^{-\frac{1}{2}}\left(\mathbf{y}_k - \mathcal{H}_k\left(\mathbf{x}_k^{\mathrm{b}} + \mathbf{B}_k^{\frac{1}{2}}\mathbf{T}^T\xi\right)\right). \quad \text{(13)}$$

The optimal solution ξ^{opt} can be obtained in few steps with the initial guess of the minimization step as: $\xi^{\mathrm{init}} = (\mathbf{I} + \mathbf{C})^{\frac{1}{2}}\mathbf{B}_k^{-\frac{1}{2}}(\mathbf{x}_k - \mathbf{x}_k^{\mathrm{b}})$.

The optimal solution in the model subspace is given by:

$$\mathbf{x}_k^{\mathrm{opt}} = \mathbf{x}_k^{\mathrm{b}} + \mathbf{B}_k^{\frac{1}{2}}(\mathbf{I} + \mathbf{C})^{-\frac{T}{2}}\xi^{\mathrm{opt}}. \quad \text{(14)}$$

The perturbation matrix is updated as:

$$\begin{aligned}
\mathbf{A}_k^{\frac{1}{2}} &= \mathbf{B}_k^{\frac{1}{2}}\left(\mathbf{I} + \mathbf{C}^{\mathrm{opt}}\right)^{-\frac{T}{2}}\ , && \text{(15a)}\\
\mathbf{C}^{\mathrm{opt}} &= (\mathbf{Z}^{\mathrm{opt}})^T\mathbf{Z}^{\mathrm{opt}}\,, && \text{(15b)}
\end{aligned}$$

where $\mathbf{Z}^{\text{opt}}$ is calculated as in equation (11b) by replacing $\mathbf{x}_k^{\text{b}}$ by $\mathbf{x}_k^{\text{opt}}$.

Of course the observation operator is not linearized and this is the main advantage of that algorithm. MLEF is designed to work efficiently with weekly non-linear observation operators (without the requirement of differentiability and without using finite-difference approximations of the Jacobian of the observation operators) in addition to linear observation operators [6]. However, it basically relies on the assumption that the posterior distribution is Gaussian, and searches for the mode (MAP) of that PDF in the optimization step, so it is not likely to give good results with multimodal distributions or much more complicated posterior PDFs as revealed in the results obtained in cases of the observation operators we use in our experiments in section (6).

3. Markov Chain Monte Carlo Sampling and the Hybrid MCMC

Markov Chain Monte Carlo (MCMC) algorithms can generally be used to calculate expectations of high dimensional distributions [17]. These methods can be used to generate samples from a fairly complicated distribution with PDF $\pi(\mathbf{x})$ by generating a Markov chain $\{\mathbf{x}(i)\}_{i\geq 0}$ for which $\pi(\mathbf{x})$ is the invariant (stationary) distribution given that $\pi(\mathbf{x})$ is known only to a multiplicative constant [17]. MCMC methods [18] were introduced by Metropolis *et. al* back in (1953) when they presented the well-known Metropolis-Hastings algorithm. MCMC methods work by generating a random walk using proposal PDF and uses what is called an "acceptance/rejection" criterion to decide whether proposed samples should be accepted as part of the samples generated or should just be rejected. These algorithms are generally powerful, but unfortunately, they may take very long time to explore the whole state space or even to converge, for more information see [19] for example. This section attempts to view the relevant theory that we used in developing the sampling filter. We start with an overview of the Hybrid version of MCMC sampling (HMCMC) then we present a detailed description and algorithm for the sampling filter and its use as a sequential data assimilation algorithm.

3.1. HMCMC sampling

Hybrid Monte Carlo (HMC) methods, also known an Hamiltonian Monte Carlo, originated in physics literature [20], are modified MCMC algorithms those try to handle the drawbacks of MCMC algorithms by incorporating a potential vector (as an auxiliary variable) and reducing the correlation between successive samples and also explore the whole space in very few steps with high probability of acceptance for generated states (samples) specially in high dimensions [21].

Suppose we want to draw samples $\{\mathbf{x}(e)\}_{e\geq 0}$ from a given probability distribution $\pi(\mathbf{x})$, that is $\mathbf{x}(e) \sim \pi(\mathbf{x})\ \forall e \geq 0$, it is essential to view the PDF $\pi(\mathbf{x})$ as a potential energy function (with $\mathbf{x}$ being viewed as a position variable) and incorporating an auxiliary variable $\mathbf{p}$ (being viewed as a momentum). The momentum is viewed as a Gaussian random vector with simple parameters (zero mean and a diagonal covariance matrix) and hence it is easy to sample from this auxiliary distribution. The algorithm proceeds by building a Markov

Chain (MC), with proposals $\mathbf{x}$ of the position variable those can be accepted or rejected based on a *Metropolis-like* acceptance/rejection rule [22].

Before summarizing the HMCMC algorithm steps, we first present its building blocks: the Hamiltonian system, the Hamiltonian (function) and the numerical integrator approximating the flow of the Hamiltonian system.

3.2. Hamiltonian equations

Hamiltonian dynamics operates on two $\mathrm{N_{var}}-$dimensional variables: position $\mathbf{x} \in \mathbb{R}^{\mathrm{N_{var}}}$, and momentum $\mathbf{p} \in \mathbb{R}^{\mathrm{N_{var}}}$, thus the phase space of points $(\mathbf{p}, \mathbf{x})$ is $\mathbb{R}^N$, $N = 2\mathrm{N_{var}}$. The total energy of the Hamiltonian system is described by a function $H(\mathbf{p}, \mathbf{x})$ that is referred to as the Hamiltonian function (or in short, the *Hamiltonian* of the system).

The evolution of the Hamiltonian system in time is described by the partial derivatives of the Hamiltonian H with respect to the state variables, that is:

$$\frac{d}{dt}\mathbf{x}_i = \frac{\partial H}{\partial p_i}, \tag{16a}$$

$$\frac{d}{dt}p_i = -\frac{\partial H}{\partial x_i}, \tag{16b}$$

for each $i = 1, 2, \ldots, \mathrm{N_{var}}$, where x_i is the i^{th} component of the vector $\mathbf{x}$, and similarly p_i is the i^{th} component of the vector $\mathbf{p}$. The time evolution of the system [22, 23] in state space is described by the flow $\{\Phi_t\}_{t \in R}$, such that $\Phi_t : \mathbb{R}^N \to \mathbb{R}^N$ maps the state of the system $(\mathbf{p}, \mathbf{x})$ throw a time interval of length t, that is $\Phi_t(\mathbf{p}(0), \mathbf{x}(0)) = (\mathbf{p}(t), \mathbf{x}(t))$ where $(\mathbf{p}(t), \mathbf{x}(t))$ describes the state of the system at an arbitrary time t, and $(\mathbf{p}(0), \mathbf{x}(0))$ is the solution of the Hamiltonian equations (16) at initial time.

In practice, numerical integrators are used to simulate the analytic flow which is almost impossible to simulate exactly [23]. The formulation of the Hamiltonian function $H(\mathbf{p}, \mathbf{x})$ is chosen based on the numerical integrator selected. The numerical integrator must preserve the characteristics of the Hamiltonian system like reversibility and conservation of volume etc, for details see [21]. Usually, the integrator of choice is Verlet/Störmer/Leapfrog (refereed to as **Verlet**) algorithm. New (higher-order) numerical integrators were presented in the literature recently as alternatives to the standard Verlet algorithm with improved characteristics, developed mainly to improve the sampling process. We will present and test the most successful ones in terms of our sampling filter along with standard Verlet integrator. All the integrators we use follow the well-known Strang's splitting formula [23].

All the integrators follow the same strategy to simulate the flow of the system; To advance the state of the system $(\mathbf{p}, \mathbf{x})$ from time $t = 0$ to time $t = T = mh$, the integrator in hand takes m steps of size h. We denote the solution of the m steps by:

$$(\mathbf{p}(T), \mathbf{x}(T)) = \Phi_T\left(\mathbf{p}(0), \mathbf{x}(0)\right). \tag{17}$$

As mentioned before, each integrator defines a formula for the Hamiltonian function, and here all the integrators used are using the same formula as in equation (18).

Next, we present the equations of the five integrators tested in this research. We start with the standard position Verlet integrator in Section 3.2.1. Three higher order integrators namely, two-stage, three-stage, and four-Stage position splitting integrators, are described. These higher-order integrators, as evident in the results of the proposed filter, are more stable and efficient than the standard Verlet that is very sensitive to the choice of the time step. For details on the derivation of these integrators see [24]. The last Integrator tested is an integrator defined by A. Beskos et al [25] mainly to work efficiently in infinite dimensional state spaces, and to avoid problems resulting from subtracting infinitely large numbers related to the total energy of the Hamiltonian system for infinite dimensional state spaces.

3.2.1. Position Verlet Integrator

The Hamiltonian function $H(\mathbf{p}, \mathbf{x})$ is defined on the special, but common, form [21]:

$$H(\mathbf{p}, \mathbf{x}) = \frac{1}{2}\mathbf{p}^T\mathbf{M}^{-1}\mathbf{p} + \mathcal{J}(\mathbf{x})\,, \tag{18}$$

where $\mathbf{M}$ is a constant positive definite symmetric matrix [23]. Based on the Hamiltonian equations:

$$\frac{d\mathbf{x}}{dt} = \frac{\partial H}{\partial \mathbf{p}} = \nabla_{\mathbf{p}} H(\mathbf{p}, \mathbf{x}) = \mathbf{M}^{-1}\mathbf{p}\,, \tag{19a}$$

$$\frac{d\mathbf{p}}{dt} = -\frac{\partial H}{\partial \mathbf{x}} = -\nabla_{\mathbf{x}} H(\mathbf{p}, \mathbf{x}) = -\nabla_{\mathbf{x}}\mathcal{J}(\mathbf{x}). \tag{19b}$$

Verlet integrator solves the Hamiltonian equations (approximates the flow) of motion through time. This integrator has two flavors those are nearly equivalent, namely, *position* and *velocity* Verlet. We will use position Verlet to unify notations along with other integrators used here.

One step of the position Verlet algorithm advances the solution of the Hamiltonian equations from time t_k to time $t_{k+1} = t_k + h$ as follows [21]:

$$\mathbf{x}_{k+1/2} = \mathbf{x}_k + \frac{h}{2}\mathbf{M}^{-1}\mathbf{p}_k\,, \tag{20a}$$

$$\mathbf{p}_{k+1} = \mathbf{p}_k - h\nabla_{\mathbf{x}}\mathcal{J}(\mathbf{x}_{k+1/2})\,, \tag{20b}$$

$$\mathbf{x}_{k+1} = \mathbf{x}_{k+1/2} + \frac{h}{2}\mathbf{M}^{-1}\mathbf{p}_{k+1}. \tag{20c}$$

The optimal selection [26] of the time step h is vaguely specified as: $h \propto (1/\mathrm{N_{var}})^{1/4}$. The experiments show that the step size should be small (close to zero) to make this integrator stable, however, it may fail, specially for high dimensionality and whenever complications are present in the target distributions.

The weakness of this simple integrator will be highlighted when used in our algorithm, specially with highly nonlinear observation operators. On the other hand, the higher-order integrators presented in Sections 3.2.2, 3.2.3, 3.2.4, have clear optimal stability intervals for the time step selection, and will show satisfactory results when used with our sampling strategy.

3.2.2. Two-stage integrator

One step of the two-stage algorithm advances the solution of the Hamiltonian equations from time t_k to time $t_{k+1} = t_k + h$ as follows [24]:

$$\begin{aligned} \mathbf{x}_1 &= \mathbf{x}_k + (a_1 h)\mathbf{M}^{-1}\mathbf{p}_k \,, && \text{(21a)} \\ \mathbf{p}_1 &= \mathbf{p}_k - (b_1 h)\nabla_{\mathbf{x}}\mathcal{J}(\mathbf{x}_1) \,, && \text{(21b)} \\ \mathbf{x}_2 &= \mathbf{x}_1 + (a_2 h)\mathbf{M}^{-1}\mathbf{p}_1 \,, && \text{(21c)} \\ \mathbf{p}_{k+1} &= \mathbf{p}_1 - (b_1 h)\nabla_{\mathbf{x}}\mathcal{J}(\mathbf{x}_2) \,, && \text{(21d)} \\ \mathbf{x}_{k+1} &= \mathbf{x}_2 + (a_2 h)\mathbf{M}^{-1}\mathbf{p}_{k+1} \,, && \text{(21e)} \end{aligned}$$

where: $a_1 = 0.21132,\ a_2 = 1 - 2a_1,\ b_1 = 0.5$.

The step size associated with this integrator has a stability interval $0 < T < 2.632$, that is, h should be chosen such that $0 < mh < 2.632$, where $T = mh$, and m is the number of steps taken by the integrator as discussed in Section 3.2.

3.2.3. Three-stage integrator

Similar to the two-stage integrator, one step of the three-stage algorithm advances the solution of the Hamiltonian equations from time t_k to time $t_{k+1} = t_k + h$ by the set of equations [24]:

$$\begin{aligned} \mathbf{x}_1 &= \mathbf{x}_k + (a_1 h)\mathbf{M}^{-1}\mathbf{p}_k \,, && \text{(22a)} \\ \mathbf{p}_1 &= \mathbf{p}_k - (b_1 h)\nabla_{\mathbf{x}}\mathcal{J}(\mathbf{x}_1) \,, && \text{(22b)} \\ \mathbf{x}_2 &= \mathbf{x}_1 + (a_2 h)\mathbf{M}^{-1}\mathbf{p}_1 \,, && \text{(22c)} \\ \mathbf{p}_2 &= \mathbf{p}_1 - (b_2 h)\nabla_{\mathbf{x}}\mathcal{J}(\mathbf{x}_2) \,, && \text{(22d)} \\ \mathbf{x}_3 &= \mathbf{x}_2 + (a_2 h)\mathbf{M}^{-1}\mathbf{p}_2 \,, && \text{(22e)} \\ \mathbf{p}_{k+1} &= \mathbf{p}_2 - (b_1 h)\nabla_{\mathbf{x}}\mathcal{J}(\mathbf{x}_3) \,, && \text{(22f)} \\ \mathbf{x}_{k+1} &= \mathbf{x}_3 + (a_1 h)\mathbf{M}^{-1}\mathbf{p}_{k+1} \,, && \text{(22g)} \end{aligned}$$

where: $a_1 = 0.11888010966548,\ a_2 = 0.5 - a_1,\ b_1 = 0.29619504261126,\ b_2 = 1 - 2b_1$.

The stability interval of the step size is $0 < T = mh < 3$ which even gives more freedom than the two-stage integrator.

3.2.4. Four-stage integrator

One step of the four-stage algorithm advances the solution of the Hamiltonian equations from time t_k to time $t_{k+1} = t_k + h$ as follows [24]:

$$\begin{aligned}
\mathbf{x}_1 &= \mathbf{x}_k + (a_1 h)\mathbf{M}^{-1}\mathbf{p}_k\,, && \text{(23a)}\\
\mathbf{p}_1 &= \mathbf{p}_k - (b_1 h)\nabla_{\mathbf{x}}\mathcal{J}(\mathbf{x}_1)\,, && \text{(23b)}\\
\mathbf{x}_2 &= \mathbf{x}_1 + (a_2 h)\mathbf{M}^{-1}\mathbf{p}_1\,, && \text{(23c)}\\
\mathbf{p}_2 &= \mathbf{p}_1 - (b_2 h)\nabla_{\mathbf{x}}\mathcal{J}(\mathbf{x}_2)\,, && \text{(23d)}\\
\mathbf{x}_3 &= \mathbf{x}_2 + (a_3 h)\mathbf{M}^{-1}\mathbf{p}_2\,, && \text{(23e)}\\
\mathbf{p}_3 &= \mathbf{p}_2 - (b_2 h)\nabla_{\mathbf{x}}\mathcal{J}(\mathbf{x}_3)\,, && \text{(23f)}\\
\mathbf{x}_4 &= \mathbf{x}_3 + (a_2 h)\mathbf{M}^{-1}\mathbf{p}_3\,, && \text{(23g)}\\
\mathbf{p}_{k+1} &= \mathbf{p}_3 - (b_1 h)\nabla_{\mathbf{x}}\mathcal{J}(\mathbf{x}_4)\,, && \text{(23h)}\\
\mathbf{x}_{k+1} &= \mathbf{x}_4 + (a_1 h)\mathbf{M}^{-1}\mathbf{p}_{k+1}\,, && \text{(23i)}
\end{aligned}$$

where: $a_1 = 0.071353913450279725904,\ a_2 = 0.26845879116123010582 0,\ a_3 = 1 - 2a_1 - 2a_2$, $b_1 = 0.1916678,\ b_2 = 0.5 - b_1$.

The stability interval is at least as equal to the interval prescribed for the three-stage integrator.

3.2.5. General integrator defined on Hilbert space

One step of this integrator advances the solution of the Hamiltonian equations from time t_k to time $t_{k+1} = t_k + h$ as follows [25]:

$$\begin{aligned}
\mathbf{p}_1 &= \mathbf{p}_k - \frac{h}{2}\mathbf{M}^{-1}\nabla_{\mathbf{x}}\mathcal{J}(\mathbf{x}_k)\,, && \text{(24a)}\\
\mathbf{x}_{k+1} &= \cos(h)\mathbf{x}_k + \sin(h)\mathbf{p}_1\,, && \text{(24b)}\\
\mathbf{p}_2 &= -\sin(h)\mathbf{x}_k + \cos(h)\mathbf{p}_1\,, && \text{(24c)}\\
\mathbf{p}_{k+1} &= \mathbf{p}_2 - \frac{h}{2}\mathbf{M}^{-1}\nabla_{\mathbf{x}}\mathcal{J}(\mathbf{x}_{k+1}). && \text{(24d)}
\end{aligned}$$

Unfortunately, this integrator suffers from the same problem of the standard position Verlet integrator that is the selection criterion of step size is vague. It should be be close to zero to achieve stability. However, it is designed with a specific purpose; working in infinite dimensional settings. As the results of the sampling algorithm shows in Section 6, with careful tuning of this integrator parameters its use results satisfactory results.

3.3. HMCMC sampling algorithm

Consider the canonical probability distribution of the state of the system $(\mathbf{p}, \mathbf{x})$ in the phase space $\mathbb{R}^N$:

$$\begin{aligned}
\propto \exp(-H(\mathbf{p},\mathbf{x})) &= \exp\left(-\frac{1}{2}\mathbf{p}^T\mathbf{M}^{-1}\mathbf{p} - \mathcal{J}(\mathbf{x})\right)\\
&= \exp\left(-\frac{1}{2}\mathbf{p}^T\mathbf{M}^{-1}\mathbf{p}\right)\ \exp(-\mathcal{J}(\mathbf{x})). && \text{(25)}
\end{aligned}$$

Clearly, the first term of this joint PDF is a Gaussian PDF with zero mean and covariance matrix $\mathbf{M}$, and fortunately, the two variables $\mathbf{p},\ \mathbf{x}$ are independent [21]. Without loss of generality, if we consider $\pi(\mathbf{x}) = \exp(-\mathcal{J}(\mathbf{x}))$ to be our target (posterior) distribution, and since $\mathbf{p}$ can be easily sampled, then we can generate a Markov Chain whose invariant distribution is $\pi(\mathbf{x})$. Any of the numerical integrators addressed above can be used to simulate the flow of the Hamiltonian system between successive states generated by the MC. The choice of the integrator does not affect the theory however it has a great impact on the performance of the sampling process. For details and gentle proof of the theory behind this argument see for example [21].

The HMC sampling algorithm works as follows: The chain starts at an initial state $\mathbf{x}_0 = \mathbf{x}(0)$.

Given a current MC state (state vector) $\mathbf{x}_k$, the transition between states (to generate a new MC state $\mathbf{x}_{k+1}$) is recursively carried out as follows:

Algorithm 1 HMCMC Sampling [21]

1: Draw a random vector $\mathbf{p}_k \sim \mathcal{N}(0, \mathbf{M})$.

2: Use one of the numerical integrators (e.g. Verlet) to advance the current state $(\mathbf{p}_k, \mathbf{x}_k)$ to obtain a *proposal* state $(\mathbf{p}^*, \mathbf{x}^*)$, i.e. $(\mathbf{p}^*, \mathbf{x}^*) = \Phi_T((\mathbf{p}_k, \mathbf{x}_k))$.

3: Evaluate the loss of energy (27, 28) based on the Hamiltonian and the integrator used, and calculate the probability:

$$a^{(k)} = 1 \wedge e^{-\Delta H}. \tag{26}$$

4: Discard both $\mathbf{p}^*,\ \mathbf{p}_k$.

5: **(Acceptance/Rejection)** Draw a uniform random variable $u^{(k)} \sim \mathcal{U}(0, 1)$:

- i- If $a^{(k)} > u^{(k)}$, accept the proposal as the next sample $\mathbf{x}_{k+1} := \mathbf{x}^*$;
- ii- If $a^{(k)} \leq u^{(k)}$, reject the proposal, and continue with the current state as the next sample, that is $\mathbf{x}_{k+1} := \mathbf{x}_k$.

6: Repeat steps 1 to 5 until sufficient and distinct samples are drawn.

The loss of total energy ΔH in (26) depends on the integrator selected and is given by:

a- For the standard Verlet, two-stage, three-stage, and four-stage integrators [21, 24]:

$$\Delta H = H(\mathbf{p}^*, \mathbf{x}^*) - H(\mathbf{p}_k, \mathbf{x}_k). \tag{27}$$

b- For the last integrator that is defined on Hilbert space [25]:

$$\begin{aligned}\Delta H &= \phi(\mathbf{x}^*) - \phi(\mathbf{x}_k) \\ &+ \frac{h^2}{8}\left(|\mathbf{M}^{-\frac{1}{2}}(-\nabla\phi(\mathbf{x}_k))|^2 - |\mathbf{M}^{-\frac{1}{2}}(-\nabla\phi(\mathbf{x}^*))|^2\right) \\ &+ h\sum_{i=1}^{m-1}\left(\mathbf{p}_k^T\left(-\nabla\phi(\mathbf{x}_k)\right)\right) \\ &+ \frac{h}{2}\left(\mathbf{p}_k^T\left(-\nabla\phi(\mathbf{x}_k)\right) + \left(\mathbf{p}^*\right)^T\left(-\nabla\phi(\mathbf{x}^*)\right)\right), \end{aligned} \tag{28}$$

where $\phi(\mathbf{x}) = -\log\left(\pi(\mathbf{x})\right)$. See [21] for more details.

Our main concerns will be the choice of the numerical integrator (along with its time step settings), and the choice of the function $\mathcal{J}(\mathbf{x})$ that represents the PDF we wish to sample from. Also, the construction of the mass matrix $\mathbf{M}$ affects the performance of the algorithm, however,. it is simply a diagonal matrix that is better selected to reflect the covariances of the posterior distribution as described in Algorithm 2.

4. Sampling Filter

Our target is to replace the analysis step in the traditional EnKF with a pure sampling procedure that brings representative ensembles from the posterior distribution that may generally be non-Gaussian. For now, lets assume, as most of the current ensemble-based data assimilation (DA) algorithms (like EnKF, and MLEF), that the posterior is Gaussian, that is:

$$\begin{aligned}\pi(\mathbf{x}) &= \mathcal{P}^{\mathrm{a}}(\mathbf{x}) \\ &\propto \exp\left(-\frac{1}{2}\left(\mathbf{x}-\mathbf{x}^{\mathrm{b}}\right)^T\mathbf{B}^{-1}\left(\mathbf{x}-\mathbf{x}^{\mathrm{b}}\right) - \frac{1}{2}(\mathbf{y}-\mathcal{H}(\mathbf{x}))^T\mathbf{R}^{-1}\left(\mathbf{y}-\mathcal{H}(\mathbf{x})\right)\right), \end{aligned} \tag{29}$$

where $\mathbf{x}^{\mathrm{b}}$ is the background state (forecast), $\mathbf{y}$ is the observation vector, and $\mathcal{H}$ is the observation operator that is generally non-linear.

Assuming the sampling will be at time t_k, our choice of $\mathcal{J}(\mathbf{x})$ is:

$$\begin{aligned}\mathcal{J}(\mathbf{x}_k) &= -\log\left(\mathcal{P}^{\mathrm{a}}(\mathbf{x}_k)\right) \\ &= \frac{1}{2}(\mathbf{x}_k-\mathbf{x}_k^{\mathrm{b}})^T\mathbf{B}_k^{-1}(\mathbf{x}_k-\mathbf{x}_k^{\mathrm{b}}) + \frac{1}{2}(\mathbf{y}_k-\mathcal{H}_k(\mathbf{x}))^T\mathbf{R}_k^{-1}(\mathbf{y}_k-\mathcal{H}_k(\mathbf{x})). \end{aligned} \tag{30}$$

Without loss of generality, we will assume that the observation operator is fixed over time, that is $\mathcal{H}_k = \mathcal{H}\ \forall k$.

To this end, we need to collect $\mathrm{N_{ens}}$ ensemble (states) members $\{\mathbf{x}_k^{\mathrm{a}}(e) \sim \mathcal{P}^{\mathrm{a}}(\mathbf{x})\}_{e=1,2,\ldots,\mathrm{N_{ens}}}$, those we can use to represent the posterior PDF and/or to calculate any moments needed to describe the state (*analysis*) of the system (e.g. the mean), or the uncertainty of the analysis estimate (e.g. The posterior error covariance matrix).

Note that the proposed sampling filter is not restricted to specific PDF and we can, in principle, remove the Gaussian assumption and proceed with any posterior PDF. In the next section we describe the proposed sampling filter as an alternative to the EnKF.

4.1. Sampling filter algorithm

The algorithm consists of two stages as most of the ensemble-based sequential DA algorithms including EnKF, namely, the *forecast* step and the *analysis* step.

Given ensemble of $\mathrm{N_{ens}}$ members, $\{\mathbf{x}^{\mathrm{a}}_{k-1}(e)\}_{e=1,2,\ldots,\mathrm{N_{ens}}}$ describing the analysis PDF of the state at time t_{k-1}, in the forecast step each ensemble member is propagated in time to the next time where observations are available (using the full model) resulting in the forecast ensemble. In the analysis step, a HMCMC algorithm is simply used to sample from the posterior PDF of the state of the assimilated system.

Algorithm 2 Sampling Filter

1: **Forecast step:** given an analysis ensemble $\{\mathbf{x}^{\mathrm{a}}_{k-1}(e)\}_{e=1,2,\ldots,\mathrm{N_{ens}}}$ at time t_{k-1}; generate the forecast ensemble:

$$\mathbf{x}^{\mathrm{b}}_{k}(e) = \mathcal{M}_{t_{k-1}\rightarrow t_k}\left(\mathbf{x}^{\mathrm{a}}_{k-1}(e)\right) \quad \forall e = 1, 2, \ldots, \mathrm{N_{ens}}\,, \tag{31}$$

where $\mathcal{M}$ represents the model dynamics.

2: **Analysis step:** Given the forecast (background) ensemble of states $\{\mathbf{x}^{\mathrm{b}}_{k}(e)\}_{e=1,2,\ldots,\mathrm{N_{ens}}}$, and an observation vector $\mathbf{y}_k$ at this time point t_k, apply the following steps:

- i- Calculate the best estimate from the forecast (e.g. the mean) and set it as an initial state $\mathbf{x}_0$ of the Markov Chain to be generated by the HMC algorithm.
- ii- Calculate the ensemble-based forecast error covariance matrix $\mathbf{B}_k$ (and possibly balance it by a fixed (or frequently updated) covariance matrix $\mathbf{B}_0$), and apply localization as in equation (6d).
- iii- Build the matrix $\mathbf{M}$, the mass matrix, as a diagonal matrix whose diagonal is taken from the diagonal of the matrix $\mathbf{B}_k$, this is believed to enhance the performance of the sampling algorithm [25, 27].
- iv- Apply the HMC algorithm presented in Section 3.3 with initial state $\mathbf{x}_0$ as in step (i), and select the last state generated after a suitable number of steps (say 30), to guarantee that selected members explores the whole state space, until the $\mathrm{N_{ens}}$ ensemble members are generated.
- v- Use the generated ensembles $\{\mathbf{x}^{\mathrm{a}}_{k}(e)\}_{e=1,2,\ldots,\mathrm{N_{ens}}}$, as a an analysis ensemble of states representing the posterior PDF $\mathcal{P}^{\mathrm{a}}_{k}(\mathbf{x})$, and use it to calculate the best estimate of the state of the system (e.g. the mean), and if desired to estimate the analysis error covariance matrix $\mathbf{A}_k$.

3: Forecast and analysis steps are repeated sequentially onto times where observation vectors (measurements) are available.

In the next section, we describe the experiment used to test the proposed algorithm.

5. Experiment Design

We have used the famous Lorenz-96 model with five different observation operators relating synthetic observation vectors to the state of the system. The number of variables is optionally selected to be 40 in our experiments, so the state vector is $\mathbf{x} = (x_1, \ldots, x_{40})^T \in \mathbb{R}^{40}$. In this section we describe the model equations and parameters, and the observation operators tested during this experiment.

5.1. Lorenz-96 model

The deterministic Lorenz-96 model [28] reads:

$$\frac{dx_i}{dt} = x_{i-1}\left(x_{i+1} - x_i\right) - x_i + F\,, \tag{32}$$

where $\mathbf{x} = (x_1, x_2, \ldots, x_{40}) \in \mathbb{R}^{40}$ is the state vector. The indices work in a circular fashion, and the forcing parameter is set to $F = 8$ in our experiment. These settings make the steady state linearly unstable, and the system chaotic [29].

5.2. Observations and observation operators

We use synthetic observation vectors generated from a reference trajectory of the model state with a specified uncertainty level. We have used six different observation operators to test the power of the sampling filter. Our choice of the observation operators reflects our desire to test the strength of the proposed algorithm with observation operators of different complexities and varying levels of non-linearity. Both quadratic and cubic observation operators were studied by Zupanski [6, 30] in the simple case of one dimensional state space.

5.2.1. Linear observation operator

The first observation operator is a linear operator $\mathbf{H}$ (short fat matrix), that is $\mathcal{H}(\mathbf{x}) = \mathbf{H}\mathbf{x}$, (we will call it a linear selector for ease of reference) that only selects a specific subset of the components of the state vector. This is an easily differentiable observation operator, that makes $\mathcal{J}(\mathbf{x})$ directly differentiable. In our experiments, we select the observation vector $\mathbf{y}$ to be:

$$\mathbf{y} = (x_1,\ x_4,\ x_7,\ \ldots,\ x_{37},\ x_{40})^T \in \mathbb{R}^{14}\,, \tag{33}$$

that is, every third component of $\mathbf{x}$, starting with the first component, is observed.

5.2.2. Quadratic observation operator

This is a quadratic observation operator. It squares the selected components by the linear observation operator (33). This is a non-linear but still also a differentiable observation operator. The observation vector reads:

$$\mathbf{y} = (x_1^2,\ x_4^2,\ x_7^2,\ \ldots,\ x_{37}^2,\ x_{40}^2)^T \in \mathbb{R}^{14}. \tag{34}$$

5.2.3. Cubic observation operator

The selected components by the linear observation operator (33) are cubed (cubic observation operator). This is a highly non-linear with more non-linearity than the quadratic selector, however, it is still a differentiable observation operator. The observation vector is:

$$\mathbf{y} = (x_1^3,\ x_4^3,\ x_7^3,\ \ldots,\ x_{37}^3,\ x_{40}^3)^T \in \mathbb{R}^{14}. \tag{35}$$

5.2.4. Magnitude observation operator

As the name suggests, this observation operator evaluates the magnitude of the components selected by the linear observation operator (33). This is our first non-differentiable observation operator used. The observation vector reads:

$$\mathbf{y} = (|x_1|,\ |x_4|,\ |x_7|,\ \ldots,\ |x_{37}|,\ |x_{40}|)^T \in \mathbb{R}^{14}. \tag{36}$$

5.2.5. Quadratic observation operator with a threshold

This observation operator is similar to the simple version used by Zupanski et al in [30]. The observation vector is given as:

$$\mathbf{y} = (x'_1,\ x'_4,\ x'_7,\ \ldots,\ x'_{37},\ x'_{40})^T \in \mathbb{R}^{14}\,, \tag{37}$$

such that:

$$x'_i = \begin{cases} x_i^2 & : x_i \geq 0.5 \\ -x_i^2 & : x_i < 0.5\,, \end{cases}$$

where again x_i refer to the components selected by the linear observation operator as in (33). This operator is highly non-linear and of course non-differentiable, and has obviously contains discontinuity in it and all its derivatives.

5.2.6. Exponential observation operator

This observation operator is again a differentiable observation operator however, we used it to test the power of the proposed algorithm in dealing with component of large magnitude and with big gab between the state variables and the observation magnitude.

The observation vector in this case reads:

$$\mathbf{y} = (e^{x'_1},\ e^{x'_4},\ e^{x'_7},\ \ldots,\ e^{x'_{37}},\ e^{x'_{40}})^T \in \mathbb{R}^{14}\,, \tag{38}$$

such that $x'_i = rx_i$ where $r \in \mathbb{R}$ is a scaling factor, and $x_i \in \mathbb{R}$ is the i^{th} component selected by the linear observation operator (33).

6. Results

Two main experiments are discussed, and both share the same model parameters settings. The two experiments use different values of the time step settings used for the integrators, which is found to have a great impact on the performance of the proposed filter, however it is not the only parameter that controls the accuracy/performance of the sampling strategy as explained in the results.

In the first experiment, a step size, $T = 0.1$ (such that $h = 0.01,\ m = 10$), is used and fixed for all integrators tested. The choice of this step size, was selected such that we guarantee that the standard position Verlet integrator gives satisfactory results with the choice of the linear observation operator, with a hope that it works well in case of using the other nonlinear observation operators. In the second experiment, the step size is tuned in a trial to make the Verlet integrator succeeds with nonlinear observation operators and the work is equalized for the other integrators.

In all experiments, 100 realizations of the sampling filter, were conducted and the RMS error is calculated and compared to the results obtained by EnKF, and MLEF. A linearized version of EnKF is used in case of nonlinear observation operators. All six observation operators described in Section 5.2 were tested. To guarantee that the Markov chain is at its stationary distribution, 200 steps are employed before starting the sampling process, then an ensemble member is chosen after each 30 steps taken by the chain. We will refer to that number of steps as inter-chain steps as it will be one of the parameters that can control the performance of the sampling filter.

The stability interval of the step size of Verlet integrator is a very small, and h should be decreased for increasing dimensionality, however, the optimal value selection rule is vague and h is still empirical [21] and should be tuned for each problem. The higher-order integrators, on the other hand, are expected to be more stable with a wider interval of stability [24, 22]. To test this claim, the step size is perturbed (20% of the selected step) used on each integration time step following the convention in [24].

6.1. Linear observation operator experiments

When the linear observation operator is used, in principle, the sampling filter gives satisfactory results comparing to both EnKF, and MLEF, except for the case when the last integrator is used as indicated in Figure (1).

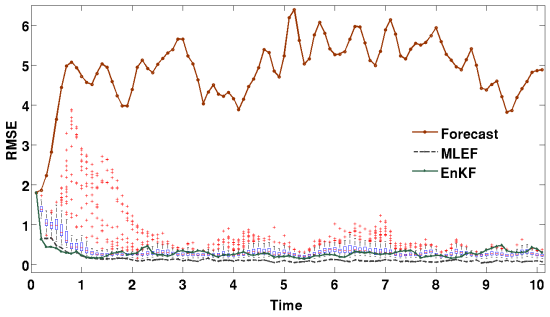

(a) Position Verlet integrator

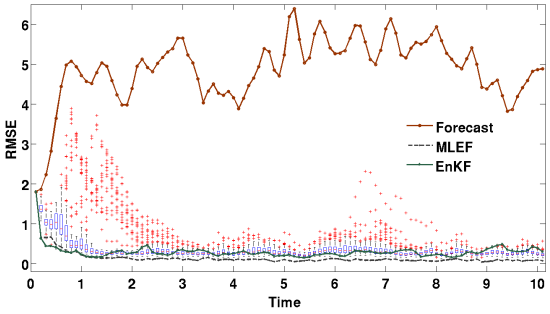

(b) Two-stage integrator

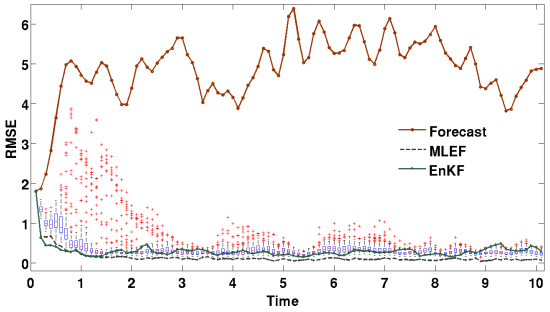

(c) Three-stage integrator

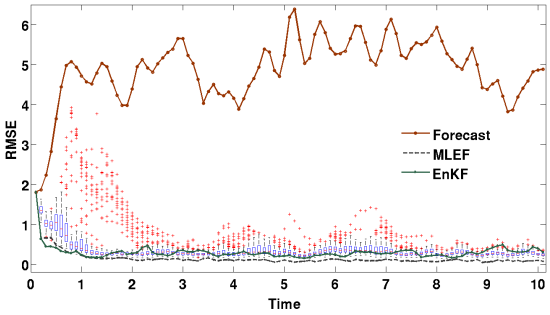

(d) Four-stage integrator

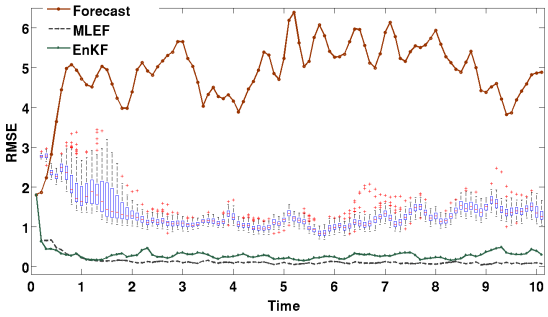

(e) Integrator defined on Hilbert Space

Figure 1: Linear (selector) observation operator is used. The integrator used is indicated under each figure. The time step for all integrators is $T = 0.1$ such that $h = 0.01$, $m = 10$. The number of inter-chain steps is 30.

The last integrator doesn't suffer much from the outliers (the red crosses) those appear when the other integrators as used. Even with this rate of RMSE that is not as small as that obtained for example by EnKF, however, the solution obtained follows the trend of the reference trajectory. this is shown for example in Figure 16. This is a property that might be useful for validation if one of the other integrators is used to avoid filter divergence.

Figure 2 shows results obtained by setting the time step parameters based on equalized work. The number of steps m is increased for two reasons, to test the capabilities of position Verlet with different step sizes while using the simplest observation operator (Linear), and

to give the best possible results using Verlet integrators so that we can make a fair choice on which integrator to use. There are several notes here; the results are enhanced (RMSE is less with smaller variation) and RMSE behavior obtained using all integrators is almost identical except for the last integrator, that is hanging the step didn't result in noticeable change in the behavior of the filter.

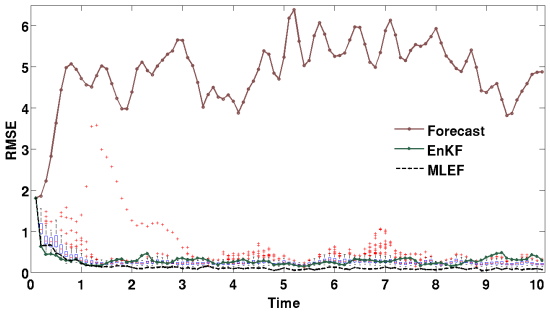

(a) Position Verlet integrator; $h = 0.01,\ m = 24$

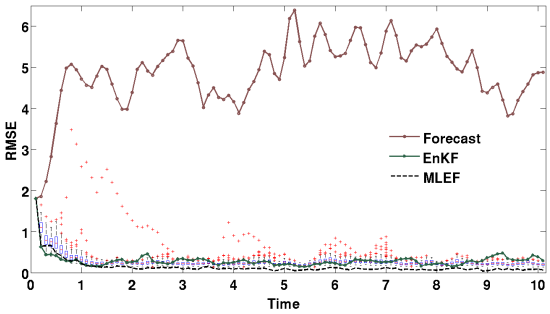

(b) Two-stage integrator; $h = 0.02,\ m = 12$

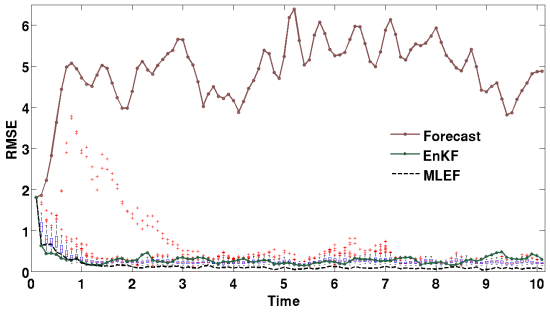

(c) Three-stage integrator; $h = 0.03,\ m = 8$

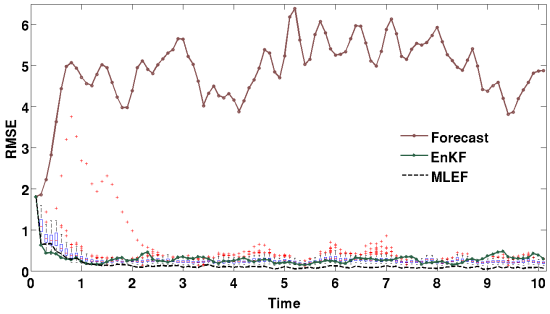

(d) Four-stage integrator; $h = 0.04,\ m = 6$

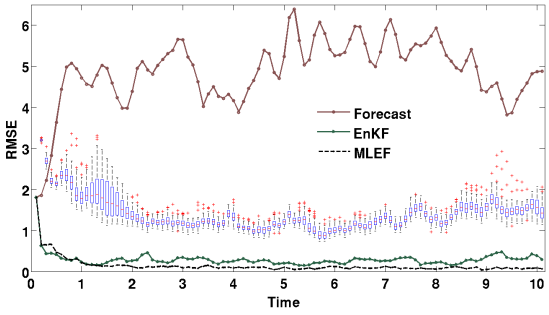

(e) Integrator defined on Hilbert space; $h = 0.01,\ m = 24$

Figure 2: Linear (selector) observation operator is used. The integrator used is indicated under each figure. The step size h and the number of steps m are indicated under each plot. The number of inter-chain steps is 30.

6.2. Quadratic observation operator experiments

The results of the quadratic observation operators are shown in Figures 3, 4. Obviously EnKF fails to converge. On the other hand, MLEF behaves as good as it did with linear observation operator. The results in Figure 3, are based on step size $h = 0.01$, $m = 10$ fixed for all integrators used in the sampling filter. The filter with Verlet integrator failed to converge and produce representative samples from the analysis PDF, however, the high-order integrators showed that, mostly the analysis converges with satisfactory RMSE comparable to that obtained by MLEF except for occasional failure represented in the plots as outliers (red crosses). In Section 6.7 we will discuss some strategies to handle such failure possibilities and avoid these outliers cases. Despite the results for the last integrator are not close to the RMSE obtained by MLEF, however, it gives better results than EnKF, and it is still suffers from outliers much less than other integrators.

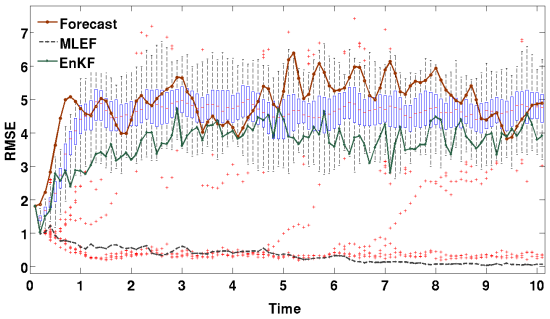

(a) Position Verlet integrator

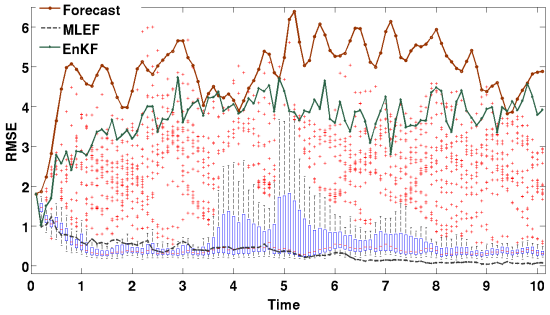

(b) Two-stage integrator

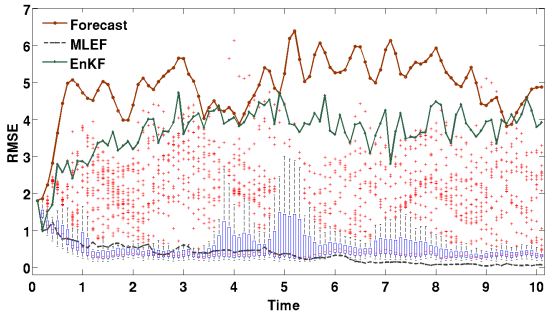

(c) Three-stage integrator

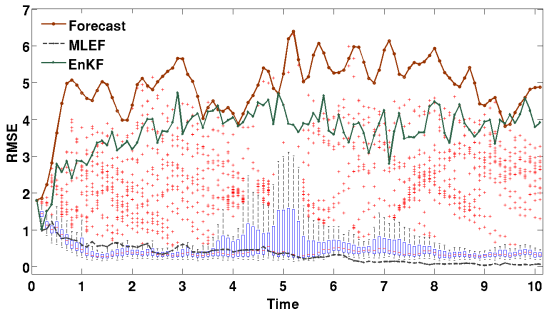

(d) Four-stage integrator

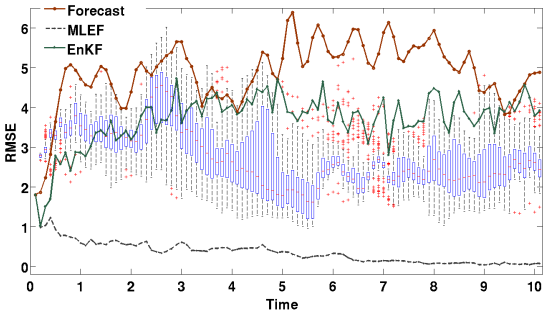

(e) Integrator defined on Hilbert space

Figure 3: Quadratic (selector) observation operator is used. The integrator used is indicated under each figure. The step size for all integrators is fixed to $T = 0.1$, such that $h = 0.01$ and $m = 10$. The number of inter-chain steps is 30.

With the aim of getting the most out of Verlet integrator in mind, the time step setting is tuned, and the work is equalized to set the parameters for the rest of integrators as shown in Figure 4. Verlet integrator results in high uncertainty in the RMSE which makes the chance of divergence of the filter very high. On the other hand the high-order integrators still gives good results but the outliers seem to increase. The integrator defined on Hilbert space fails completely giving extremely large RMSE in many cases. It is clear that the step size of the integrator should be tuned independently from both Verlet and Hilbert integrator, specially with this nonlinear observation operator. Based on our experiments

and experience, we believe that each of the integrators, except Verlet, can be tuned to give very satisfactory results. Verlet integrators either makes the filter diverge or at least its behavior is unpredictable.

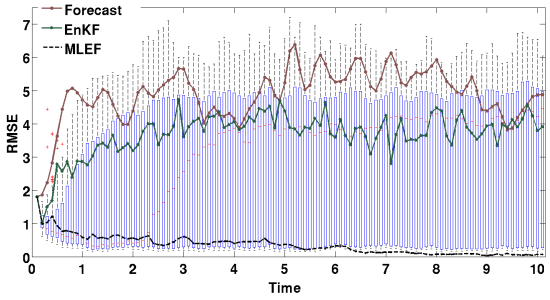

(a) Position Verlet integrator; $h = 0.01,\ m = 40$

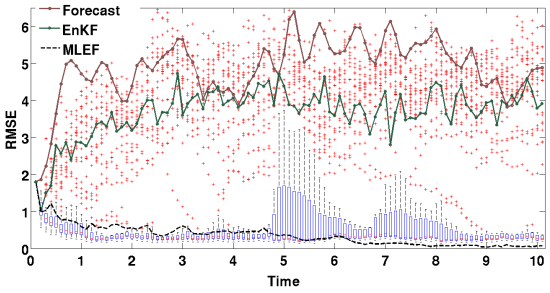

(b) Two-stage integrator; $h = 0.02,\ m = 20$

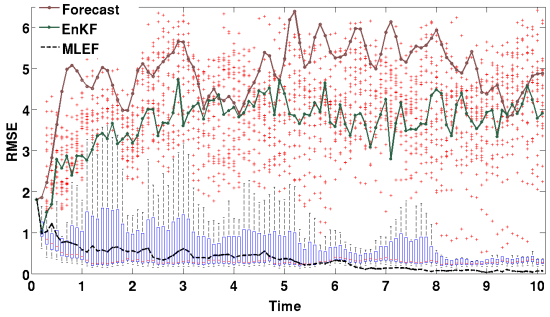

(c) Three-stage integrator; $h = 0.03,\ m = 13$

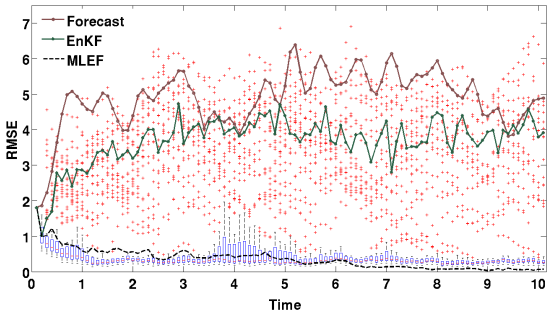

(d) Four-stage integrator; $h = 0.04,\ m = 10$

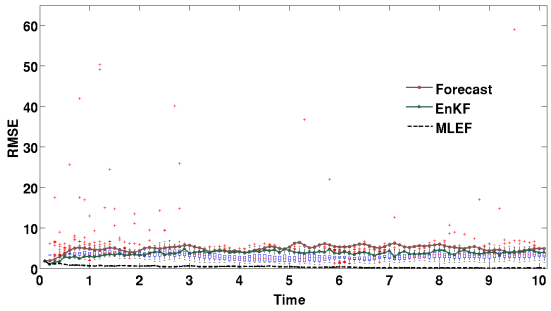

(e) Integrator defined on Hilbert space; $h = 0.01,\ m = 40$

Figure 4: Quadratic (selector) observation operator is used. The integrator used is indicated under each figure. The step size h and the number of steps m are indicated under each plot. The number of inter-chain steps is 30.

6.3. Cubic observation operator experiments

Figures 5,6 reveal that both EnKF, and MLEF fails due to high non-linearity of the observation operator and/or the dimensionality of the problem. The sampling filter with position Verlet integrator fails to converge, however, the results gets better by increasing the

stage of the integrator, for example, we can see that using four-stage integrator, we get very satisfactory results in compared to the two, and three stage integrators. The last integrator gives result very similar to those obtained in case when the linear observation operator was used. This means that each of the high-order integrators can be tuned to give results as good as those resulting from using four-stage integrator.

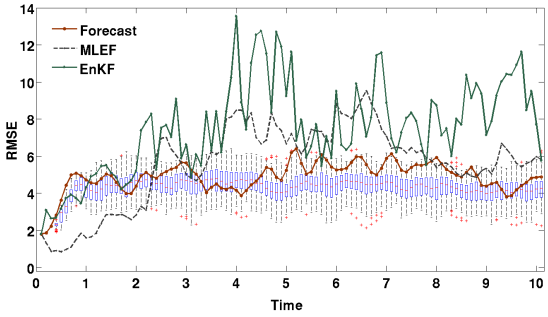

(a) Position Verlet integrator

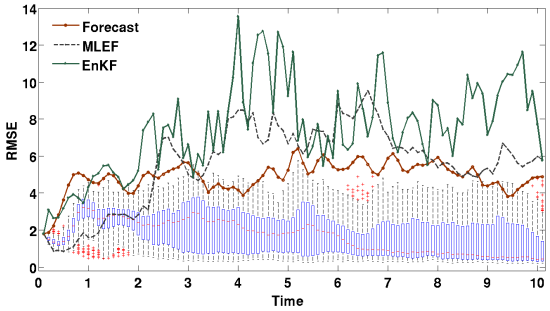

(b) Two-stage integrator

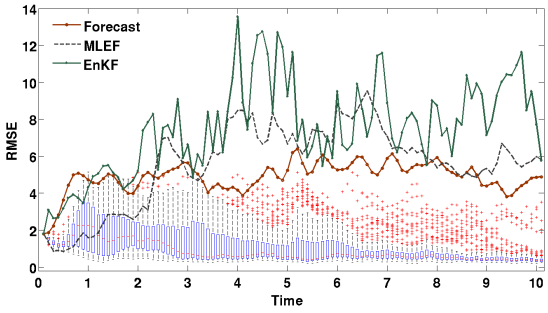

(c) Three-stage integrator

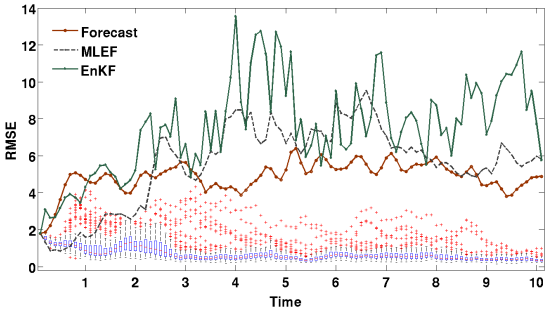

(d) Four-stage integrator

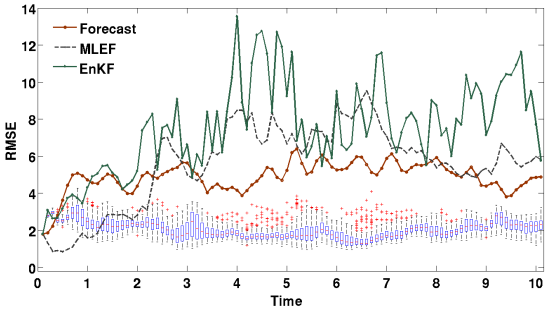

(e) Integrator defined on Hilbert space

Figure 5: Cubic (selector) observation operator is used. The integrator used is indicated under each figure. The step size for all integrators is fixed to $T = 0.1$, such that $h = 0.01$ and $m = 10$. The number of inter-chain steps is 30.

Unfortunately, this is not the case with the simple position Verlet. The best results we could by tuning the step size for Verlet integrator is shown in Figure 6. More work is needed

with finer step size to force the sampling filter with Verlet integrator to converge, but there is a big chance of divergence as revealed in the boxplot in Figure 6(a). The high-order integrators still give good results, but reducing the step size degraded the performance of the four stage integrator slightly (and consequently two and three stage integrators of course as work is equalized here). As shown in Figure 6(e), Hilbert integrator resulted in extremely large RMSE with this setting of step size. Again, it is highly advisable to tune the step size of this integrator independently from Verlet integrator in case it has to be used (e.g. with very large dimensions or observations very large magnitudes.

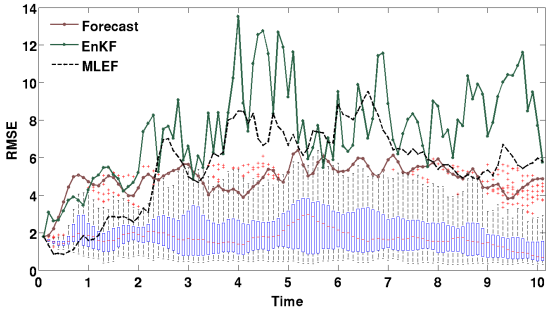

(a) Position Verlet integrator; $h = 0.001,\ m = 40$

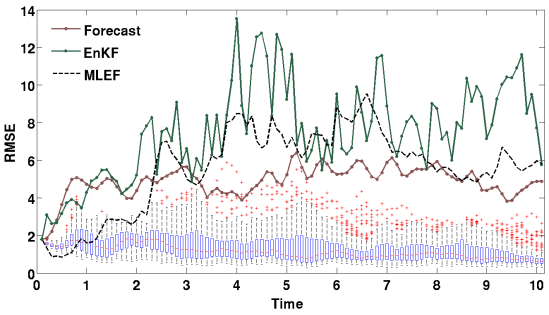

(b) Two-stage integrator; $h = 0.002,\ m = 20$

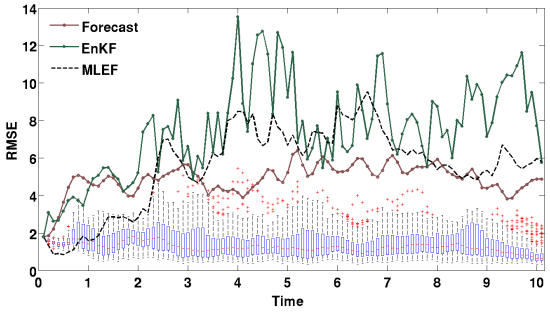

(c) Three-stage integrator; $h = 0.003,\ m = 13$

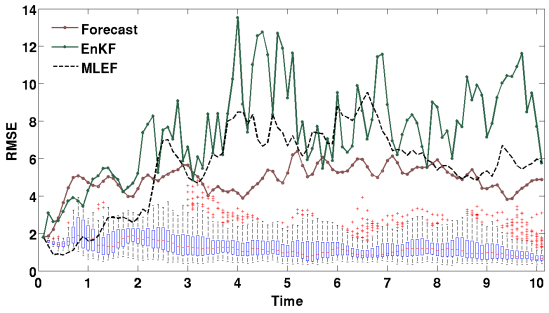

(d) Four-stage integrator; $h = 0.004,\ m = 10$

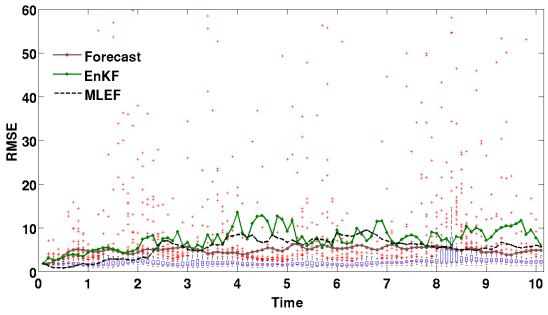

(e) Integrator defined on Hilbert space; $h = 0.001,\ m = 40$

Figure 6: Cubic (selector) observation operator is used. The integrator used is indicated under each figure. The step size h and the number of steps m are indicated under each plot. The number of inter-chain steps is 30.

6.4. Absolute value observation operator experiments

The Tangent linear (Jacobian) of this observation operator is taken as the sign of the measured components of the state vector. As obvious in Figure 7, MLEF succeeded as expected, since the observation operator is weekly non-linear. The sampling filter using Hilbert integrator shows improvement over the forecast, but it fails to achieve the same low level of RMSE obtained from MLEF or even EnKF which takes time to converges. Verlet and the high-order integrators behaves almost identically, which means that we should favor

Verlet if we can deal with the outliers. One thing to note here is that the distribution of outliers is similar to those observed with Quadratic observation operator, and again we will discuss how to deal with this occasional divergence in Section 6.7.

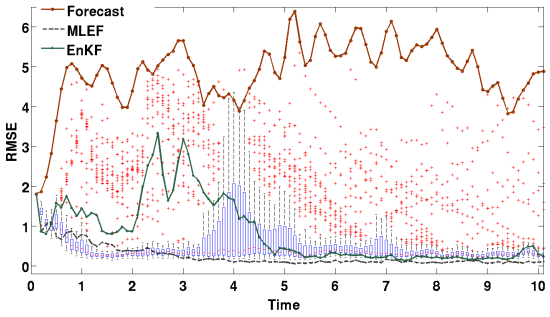

(a) Position Verlet integrator

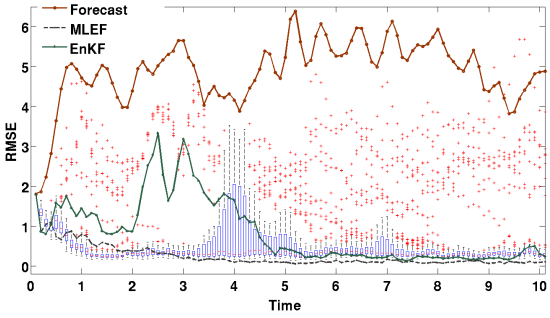

(b) Two-stage integrator

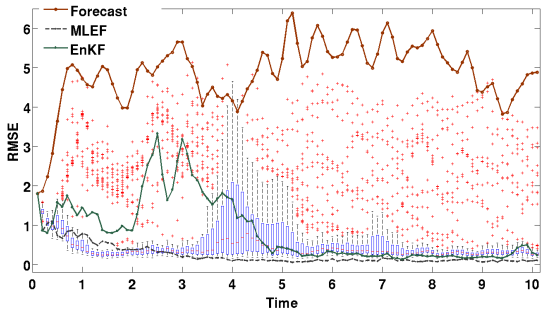

(c) Three-stage integrator

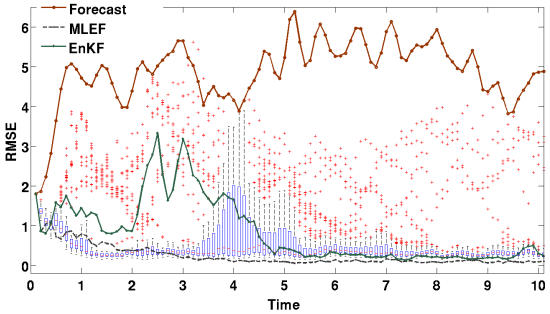

(d) Four-stage integrator

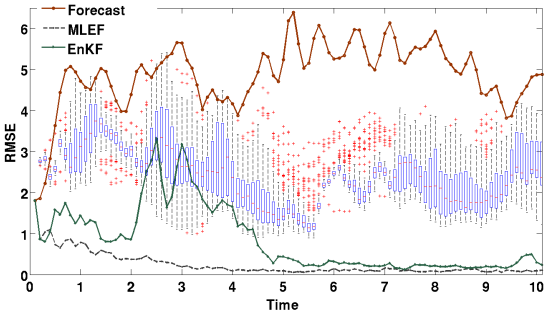

(e) Integrator defined on Hilbert space

Figure 7: Absolute value (magnitude selector) observation operator is used. The integrator used is indicated under each figure. The step size for all integrators is fixed to $T = 0.1$, such that $h = 0.01$ and $m = 10$. The number of inter-chain steps is 30.

Increasing the step size doesn't seem to change the behavior of Sampling filter with Verlet integrator, however, the results obtained using high-order integrators, based on equalized work, are worse and mimic the behavior of EnKF in times where it tend to diverge. Figure 8 shows these results. The use of Hilbert integrator may results in extremely large RMSE,

however, if this happens it recovers. This might be an advantage in its own as we can use it to validate ensembles obtained based on use of other integrators periodically.

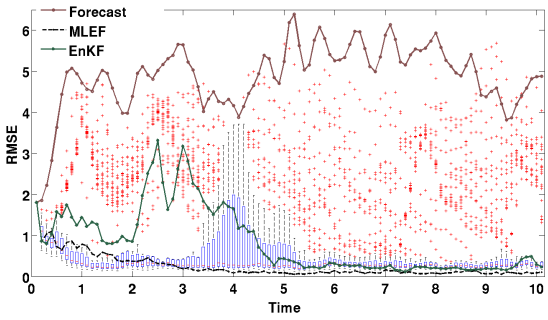

(a) Position Verlet integrator; $h = 0.01,\ m = 24$

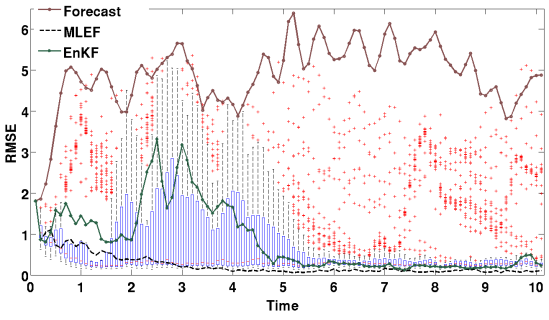

(b) Two-stage integrator; $h = 0.02,\ m = 12$

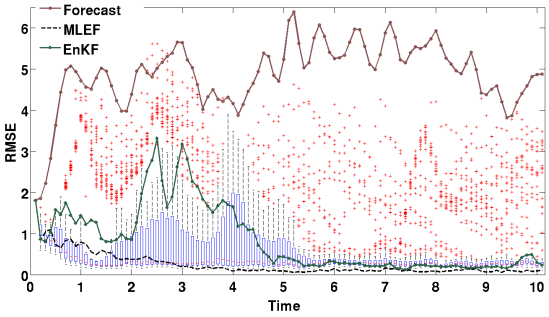

(c) Three-stage integrator; $h = 0.03,\ m = 8$

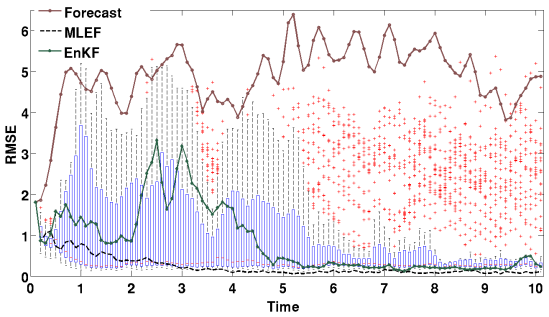

(d) Four-stage integrator; $h = 0.04,\ m = 6$

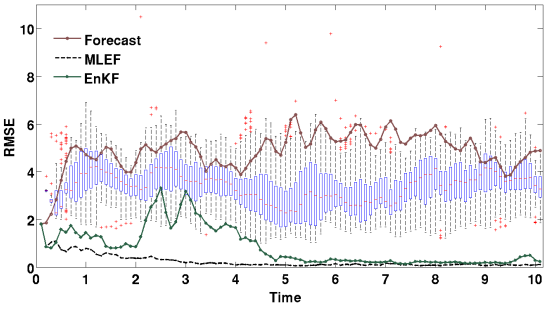

(e) Integrator defined on Hilbert space; $h = 0.01,\ m = 24$

Figure 8: Absolute value (magnitude selector) observation operator is used. The integrator used is indicated under each figure. The step size h and the number of steps m are indicated under each plot. The number of inter-chain steps is 30.

6.5. Quadratic observation operator (with a threshold) experiments

Despite MLEF was tested with one dimensional models with this version of observation operator [30], we can see that it completely fails with high dimensionality. Figures 9,10, show that using Verlet integrator again fails due to the high non-linearity of the observation

operator. The high order integrator shows exceptional results and the sampling filter reaches the level of RMSE obtained in case of linear observation operator. We can conclude that the ensemble produced by the filter is representative to the posterior PDF as both the mean and the covariance are incorporated in the analysis steps. The chance of outliers to appear is very small and decreases by using higher-order integrators. Hilbert integrator performs as expected and gives fair results based on its results with previous operators using the same time step settings.

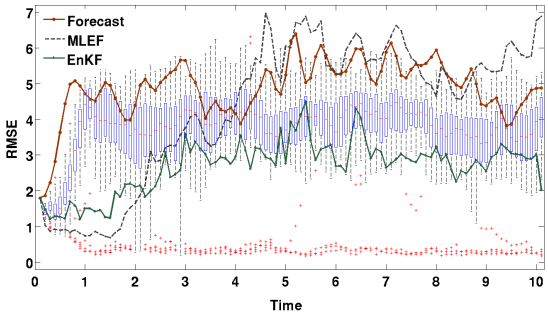

(a) Position Verlet integrator

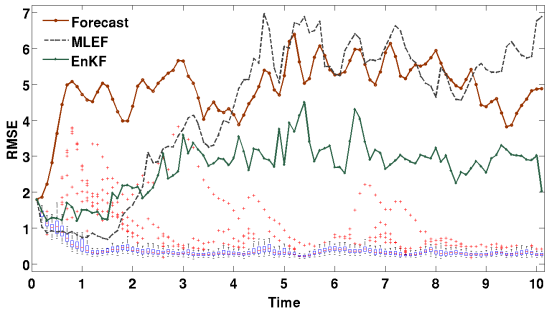

(b) Two-stage integrator

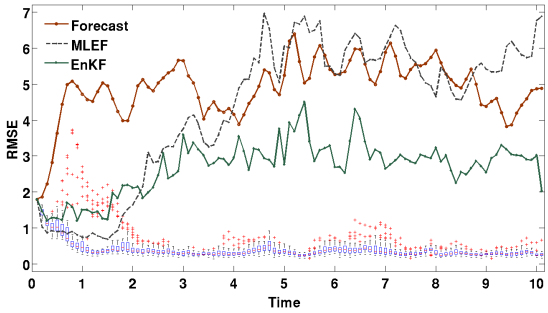

(c) Three-stage integrator

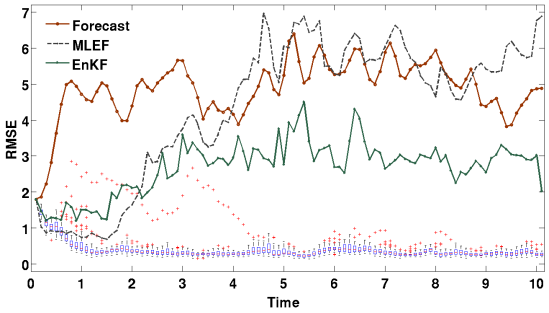

(d) Four-stage integrator

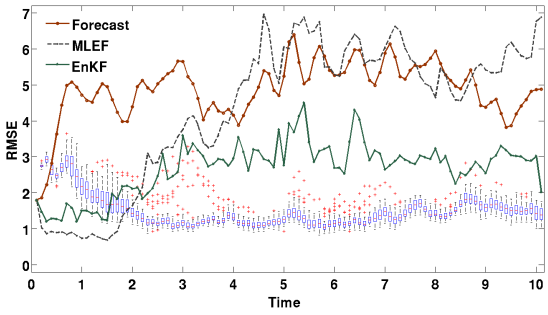

(e) Integrator defined on Hilbert space

Figure 9: Quadratic observation operator with threshold value is used. The integrator used is indicated under each figure. The step size for all integrators is fixed to $T = 0.1$, such that $h = 0.01$ and $m = 10$. The number of inter-chain steps is 30.

By increasing step size and changing time step based on equalized work, we get the results viewed in Figure 10. It is obvious that Four stage operator is superior with such level of non-linearity as it suffers the less of outliers, and gives very small RMSE. However, Verlet integrator gives satisfactory results and may perform better. Hilbert integrator on the other hand, may result in high RMSE but it can recover even if the analysis is very far from the true solution even if the wrong step size is selected.

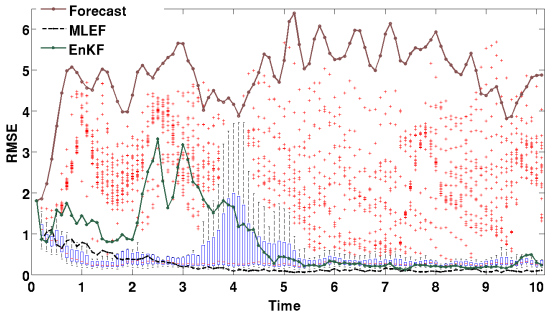

(a) Position Verlet integrator; $h = 0.01,\ m = 24$

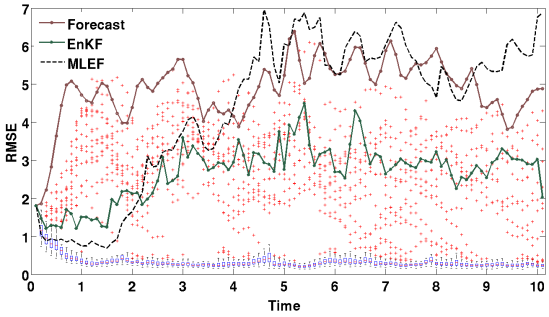

(b) Two-stage integrator; $h = 0.02,\ m = 12$

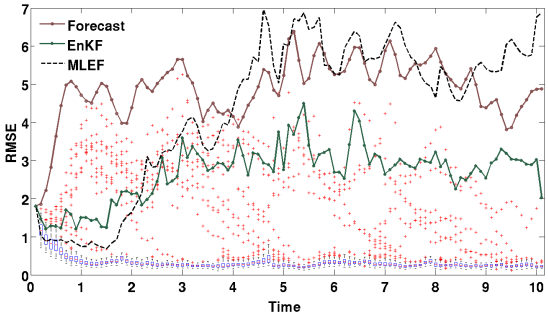

(c) Three-stage integrator; $h = 0.03,\ m = 8$

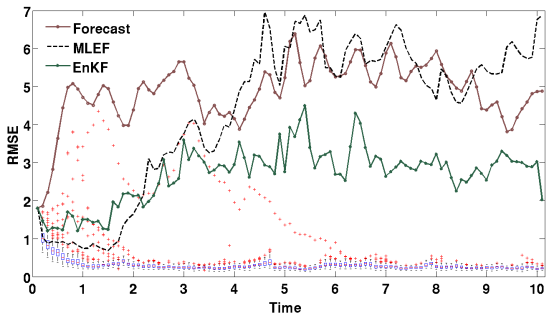

(d) Four-stage integrator; $h = 0.04,\ m = 6$

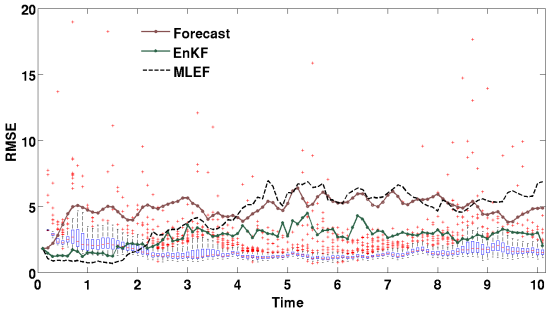

(e) Integrator defined on Hilbert space; $h = 0.01,\ m = 24$

Figure 10: Quadratic Observation Operator with threshold value is used. The integrator used is indicated under each figure. The step size h and the number of steps m are indicated under each plot. The number of inter-chain steps is 30.

The Jacobian of this observation operator is approximated using finite differences. Alternatives will be tested in the future.

6.6. Exponential observation operator (with factor $r = 0.2$) experiments

This observation operator is differentiable however, the small perturbations in the state might result in relatively large change in the measurement obtained. The results given in Figures 11,11, show that the sampling filter achieves its goal in such conditions and beat both MLEF and EnKF. The performance of the sampling filter in this experiment is much like its performance in case of using linear observation operator in both experiments conducted with different time steps of the integrators.

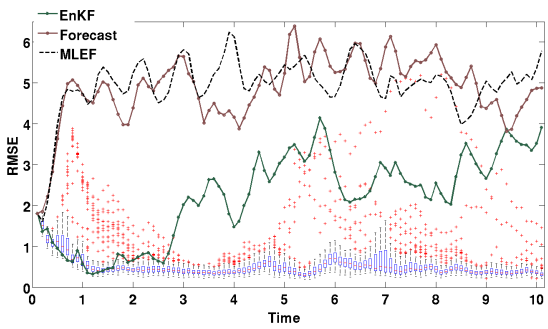

(a) Position Verlet integrator

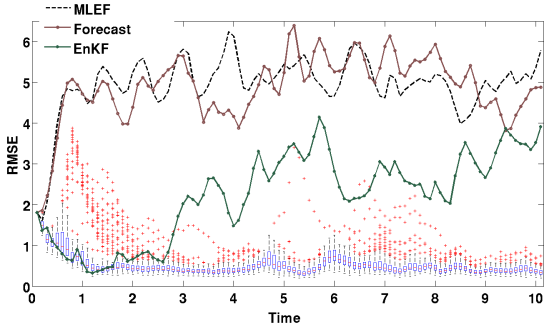

(b) Two-stage integrator

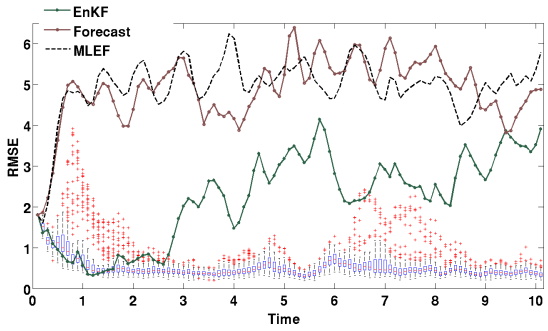

(c) Three-stage integrator

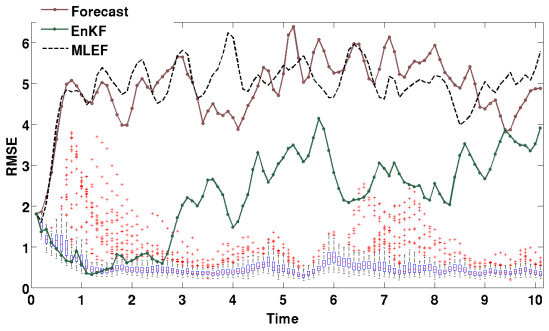

(d) Four-stage integrator

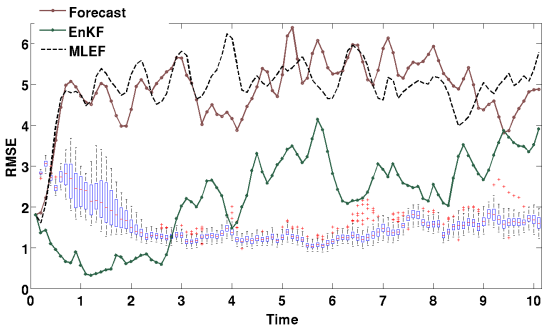

(e) Integrator defined on Hilbert space

Figure 11: Exponential (selector) observation operator is used with a factor $r = 0.2$. The integrator used is indicated under each figure. The step size for all integrators is fixed to $T = 0.1$, such that $h = 0.01$ and $m = 10$. The number of inter-chain steps is 30.

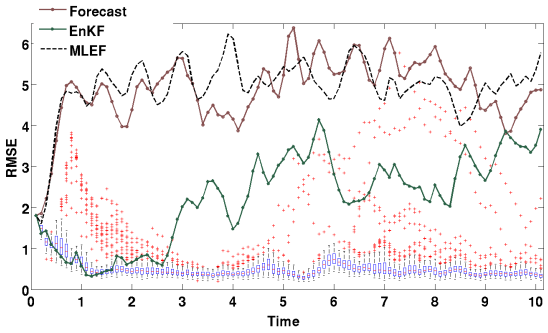

(a) Position Verlet integrator; $h = 0.01,\ m = 16$

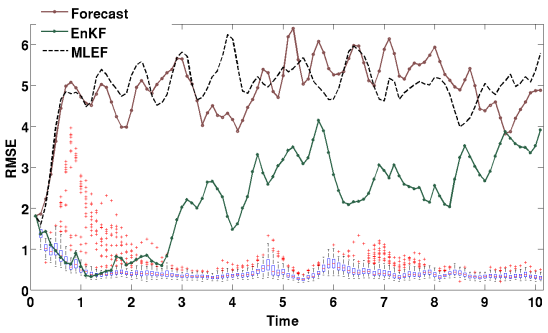

(b) Two-stage integrator; $h = 0.02,\ m = 8$

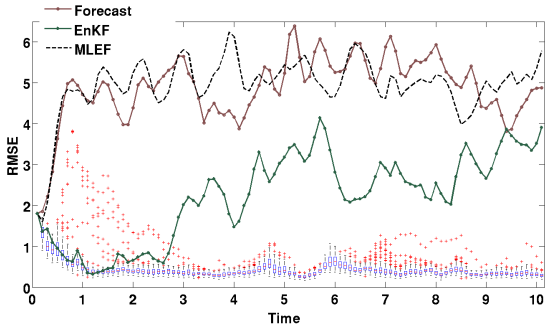

(c) Three-stage integrator; $h = 0.03,\ m = 6$

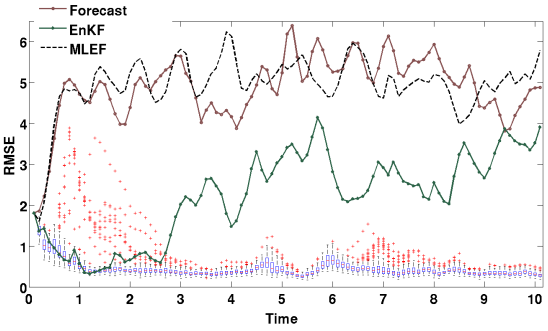

(d) Four-stage integrator; $h = 0.04,\ m = 4$

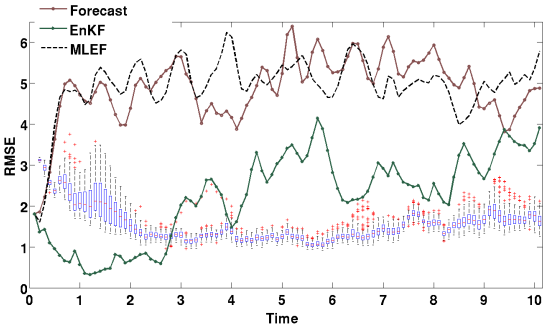

(e) Integrator defined on Hilbert space; $h = 0.01,\ m = 16$

Figure 12: Exponential Observation Operator with factor $r = 0.2$ is used. The integrator used is indicated under each figure. The step size h and the number of steps m are indicated under each plot. The number of inter-chain steps is 30.

6.7. Number of steps in MC between successive state selections

In this section we discuss how we can prevent outliers (filter divergence) that happened, specially in case of quadratic observation operator. The most basic idea is to tune the time step of the integrator. For example, the Quadratic observation operator is retested with the high-order integrators with the step sizes adopted by Blanes [24] but still the outliers possibility is evident. We need to give the filter more chance to explore the state space and

updates the state selected by the chain. Figure 13 shows the mean and standard deviation of RMSE resulted from applying the sampling filter with different number of steps taken by the Markov Chain between successive selection of ensemble states. We can see that optimizing the number of inter-steps (at slightly more or less fixed cost) can in principle result in great enhancement in both performance and confidence in the results obtained by the filter. In fact we can see that setting the number of inter-chain steps in the chain to 30 is not the best choice with this observation operator, and we can get a dramatically better results by increasing in to 40 for example as in Figure 14 that shows RMS error distribution obtained from using three stage integrator with the sampling filter.

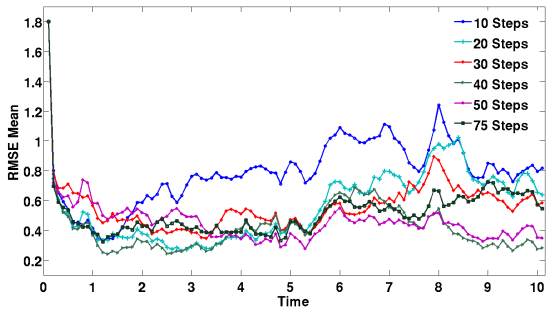

(a) RMSE mean: two-stage integrator; $h = 2/\mathrm{N_{var}}$, $m = \mathrm{N_{var}}$

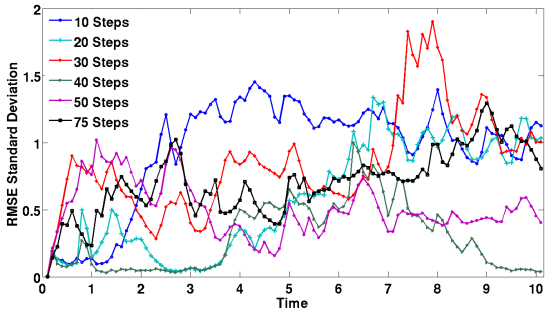

(b) RMSE standard deviation: two-stage integrator; $h = 2/\mathrm{N_{var}}$, $m = \mathrm{N_{var}}$

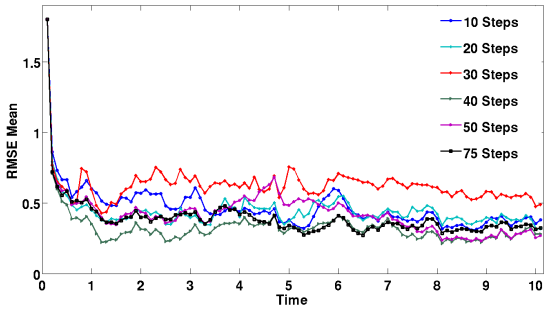

(c) RMSE mean: three-stage integrator; $h = 3/\mathrm{N_{var}}$, $m = \mathrm{N_{var}}/2$

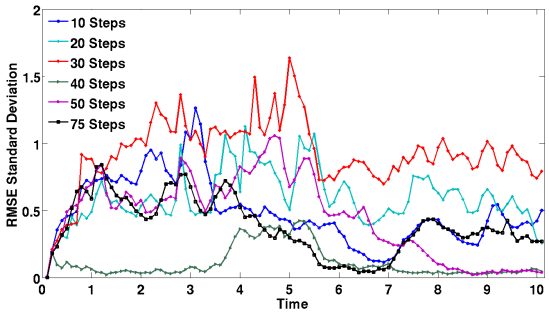

(d) RMSE standard deviation: three-stage integrator; $h = 3/\mathrm{N_{var}}$, $m = \mathrm{N_{var}}/2$

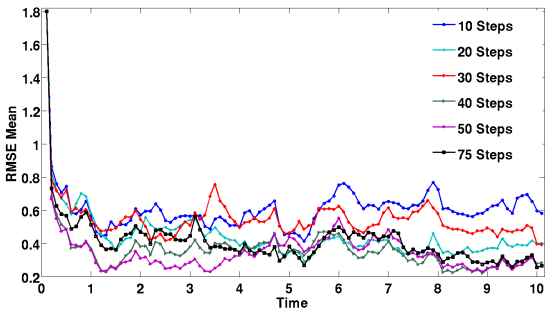

(e) RMSE mean: four-stage integrator; $h = 4/\mathrm{N_{var}}$, $m = \mathrm{N_{var}}/2$

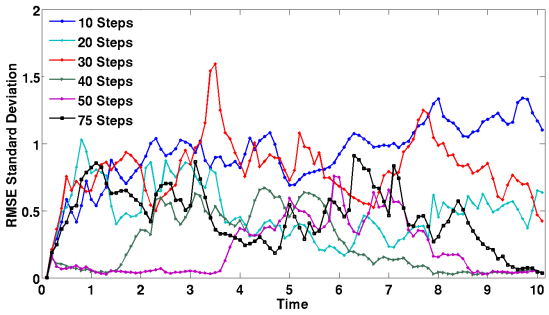

(f) RMSE standard deviation: two-stage integrator; $h = 4/\mathrm{N_{var}}$, $m = \mathrm{N_{var}}/2$

Figure 13: The mean and standard deviation of RMS error are plotted using the quadratic observation operator for different MC number of inter-chain steps. The step size h and the number of steps m are indicated under each plot, $\mathrm{N_{var}} = 40$ is the dimension of the state vector.

As revealed in the plots, we can see that controlling the number of inter-steps in the chain may overcome the problem of outliers that occurred before. For example, the RMSE resulting from choosing the Three Stage integrator, and selecting the number of inter-steps in the MC to be 40 instead of 30, we get rid of outliers as revealed in Figure 14. We can consider this result as well as controlling the step size parameters to enhance the performance

of the filter.

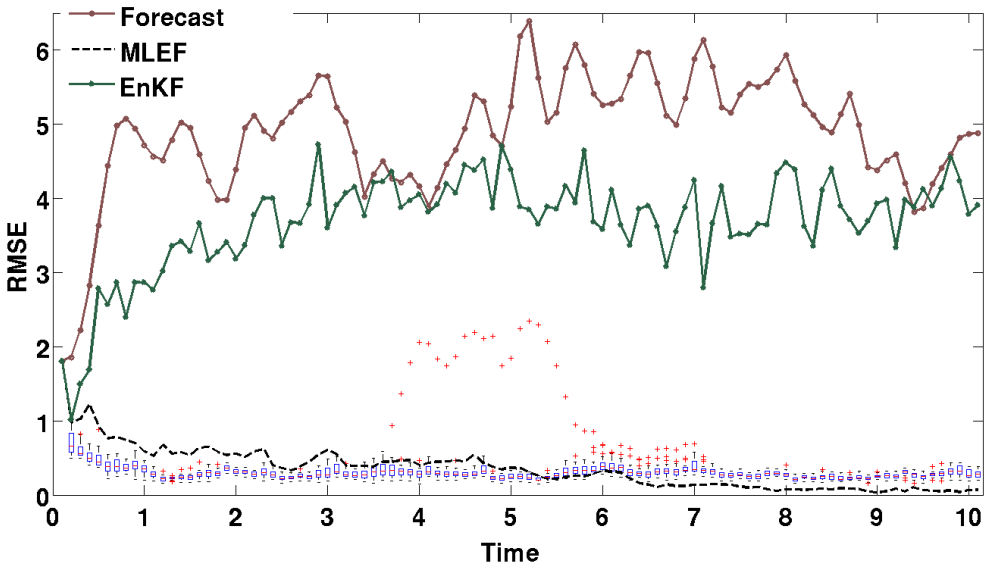

Figure 14: RMS error of the sampling filter using three-stage integrator with $h = 3/\mathrm{N_{var}}$, $m = \mathrm{N_{var}}/2$. The number of inter-chain steps is 40.

In addition to controlling both the time step setting of the integrator, and tuning the number of steps of the chain, we can use the Hilbert integrator (with tuned step size) to validate the ensembles obtained using Verlet or any of the high-order integrators periodically as it suffers the less from outliers and it recovers if it does. The naive solution of course is possible, that is to run the assimilation process several times and exclude outlier states and create a combined ensemble. Resetting the filter periodically, might be considered as an alternative for validating the ensembles.

These alternatives will be inspected in depth in future work while being applied to more complicated models. However, we can conclude that, in principle, we can almost get the desired performance by tuning the parameters of the filter based on the problem in hand and based on the available computational capabilities.

6.8. Adding more difficulty

We have also tested the sampling filter capabilities in a very tough condition. We re-defined the exponential observation operator with a factor of $r = 0.5$ Which results in observations with significantly large magnitudes, roughly from $e^{-3.7}$ to $e^{6.2}$, this results in a wide gab between the observations and the equivalent state even with small observation uncertainty. Small perturbation in the state variables causes dramatic increase in the corresponding measurements. EnKF, and MLEF totally failed, so they are not included in the figures in this experiment.

In this case, all integrators tend to fail unless we increase the number of steps taken by the integrator which might bring instability to the integrator. In fact, Verlet, two and four

stage integrators always tended to fail with any parameter setting. However,the three stage surprisingly behaved differently from two and four stage integrators even with equalized work, and started to produce very satisfactory results with larger step size as shown in Figure 15(a).

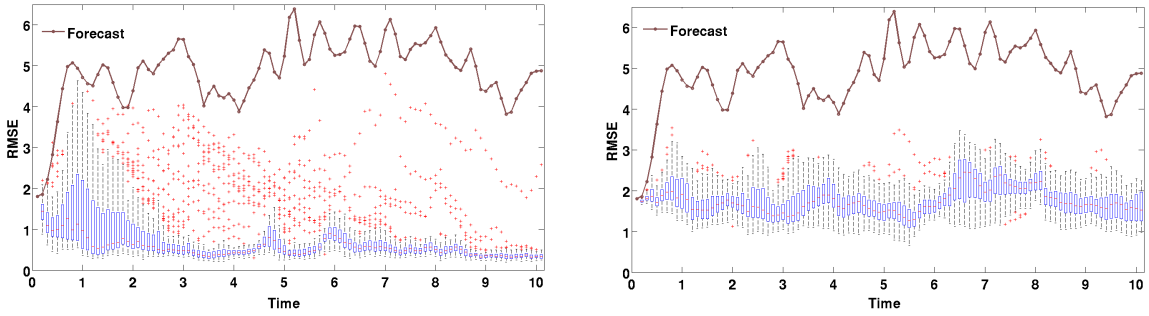

(a) Three-stage integrator; $h = 0.01,\ m = 60$ (b) Four-stage integrator; $h = 0.001,\ m = 30$

Figure 15: Exponential Observation Operator with factor $r = 0.5$ is used. The integrator used is indicated under each figure. The step size h and the number of steps m are indicated under each plot. The number of inter-chain steps is 30.

Fortunately, the integrator defined on Hilbert space still operates at its performance level achieved on using the simpler observation operators; see Figure 16. Despite the fact that the RMSE achieved using the integrator defined on Hilbert space looks relatively high, we can argue that this level might be acceptable if we have to deal with infinitely large dimensionality/magnitudes if all other integrators fail. The results in Figure 16 show the solution for selective components of the state vector $\mathbf{x}$ obtained based on this integrator.

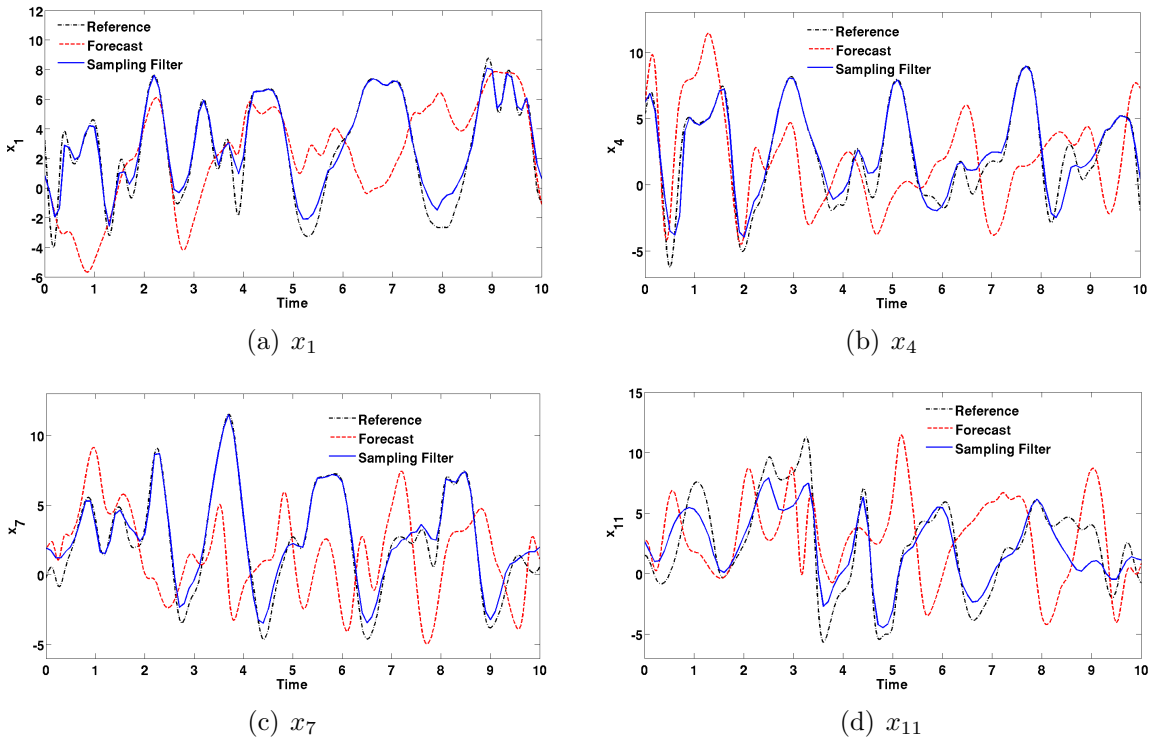

(a) x_1 (b) x_4

(c) x_7 (d) x_{11}

Figure 16: Integrator defined on Hilbert space is used; $h = 0.001,\ m = 30$. The components x_1, x_4, x_7, x_{11} of the state vector $\mathbf{x}$ are plotted. The number of inter-chain steps is 30.

Also, we plot these variables for the case where three stage integrator, see Figure 17 which required large number of steps to achieve that results due to the large magnitude of observations.

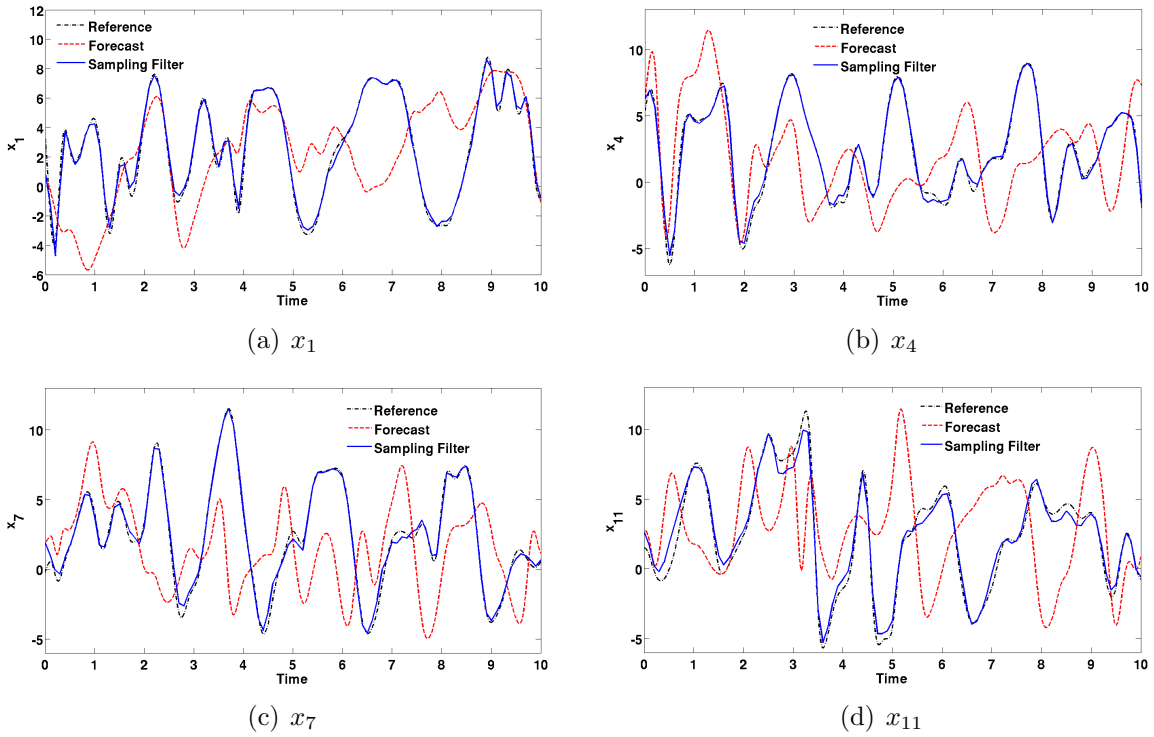

(a) x_1 (b) x_4

(c) x_7 (d) x_{11}

Figure 17: Three-stage integrator is used; $h = 0.01,\ m = 60$. The components x_1, x_4, x_7, x_{11} of the state vector $\mathbf{x}$ are plotted. The number of inter-chain steps is 30.

We can see that, at much less cost, the Hilbert integrator can be used in this case or at least used periodically to validate results obtained by using three stage integrator to deal with the chance of outliers to occur.

The RMS error statistics, calculated over the time interval $8 \leq t \leq 10$, for all the experiments presented before, are displayed in Tables 1, 2.

The average and standard deviation of the RMS errors, calculated over the time interval $8 \leq t \leq 10$, for experiments with fixed step size used for all integrators, are displayed in Tables 3, 4.

7. Conclusion and Future Work

The sampling filter is presented with application to the Lorenz-96 model with various observation operators of different levels of complexity and non-linearity. The filter replaces the analysis scheme by a pure sampling strategy.

The proposed filter adopts of the HMCMC sampling technique to collect a representative ensemble from the posterior distribution of the system state. The sampling filter completely avoid the calculation of tangent linear models or adjoints required by variational methods and works directly with nonlinear observation operators. The formulation of the algorithm is simple and it is directly applicable to many operational models and/or observation operators of different complexity.

The collected samples can be used to describe the posterior distribution in different ways. In case of Gaussian distribution it is reasonable to use the mean of the ensemble as an estimate of the state which is also a MAP in such case. The analysis error covariance matrix can be estimated from the collected ensemble members to quantify the uncertainty of the estimated analysis state.

It should be noted that the sampling filter competes with the results of both EnKF and MLEF for linear observations. This makes the proposed filter a good candidate to be used to replenish dead ensemble members in any parallel implementation of the EnKF. For nonlinear observations the results are very promising and even satisfactory results can be obtained in cases where EnKF and MLEF completely fail.

The filter is flexible and, in principle, is general and can be applied in cases of non-Gaussian PDFs and/or nonlinear observation operator with careful tuning of the parameters of the algorithm, specially, the integrator time step and the number of steps in Markov chain between successive selection of ensemble members.

In future work, much attention will be given to parameter tuning of the filter and application to operational models of high-resolution.

References

[1] E. Kalnay, Atmospheric modeling, data assimilation and predictability, Cambridge University Press, 2002.

[2] G. Evensen, Sequential data assimilation with a nonlinear quasi-geostrophic model using Monte Carlo methods to forecast error statistics, Journal of Geophysical Research 99 (C5) (1994) 10143–10162.

[3] M. Tippett, J. Anderson, C. Bishop, Ensemble square root filters, Monthly Weather Review 131 (2003) 1485–1490.

[4] G. Burgers, P. J. Van Leeuwen, G. Evensen, Analysis scheme in the ensemble Kalman filter, Monthly Weather Review 126 (1998) 1719–1724.

[5] P. Houtekamer, H. Mitchell, Data assimilation using an ensemble Kalman filter technique, Monthly Weather Review 126 (1998) 796–811.

[6] M. Zupanski, Maximum likelihood ensemble filter: theoretical aspects, Monthly Weather Review 133 (6).

[7] S. E. Cohn, An introduction to estimation theory, J. Meteorol. Soc. Jpn 75 (1997) 257–288.

[8] R. Kalman, A new approach to linear filtering and prediction problems, Transaction of the ASME-Journal of Basic Engineering 82 (1960) 35–45.

[9] R. E. Kalman, R. S. Bucy, New results in linear filtering and prediction theory, Journal of basic engineering 83 (1) (1961) 95–108.

[10] A. H. Jazwinski, Stochastic processes and filtering theory, Academic Press, New York, 1970.

[11] P. Houtekamer, H. L. Mitchell, Ensemble Kalman filtering, Quarterly Journal of the Royal Meteorological Society 131 (613) (2005) 3269–3289.

[12] E. G., Data assimilation: the ensemble Kalman filter, Springer, Berlin, 2007.

[13] P. Houtekamer, H. Mitchell, A sequential ensemble Kalman filter for atmospheric data assimilation, Monthly Weather Review 129 (2001) 123–137.

[14] T. M. Hamill, J. S. Whitaker, Distance-dependent filtering of background error covariance estimates in an ensemble Kalman filter, Monthly Weather Review 129 (2001) 2776–2790.

[15] A. C. Lorenc, Analysis methods for numerical weather prediction, Quarterly Journal of the Royal Meteorological Society 112 (474).

[16] M. Fisher, P. Courtier, Estimating the covariance matrices of analysis and forecast error in variational data assimilation, European Center for Medium-Range Weather Forecasts, 1995.

[17] R. M. Neal, Probabilistic inference using Markov chain Monte Carlo methods.
[18] N. Metropolis, A. W. Rosenbluth, M. N. Rosenbluth, A. H. Teller, E. Teller, Equation of state calculations by fast computing machines, The journal of chemical physics 21.
[19] L. Tierney, Markov chains for exploring posterior distributions, the Annals of Statistics (1994) 1701–1728.
[20] S. Duane, A. D. Kennedy, B. J. Pendleton, D. Roweth, Hybrid Monte Carlo, Physics letters B 195 (2) (1987) 216–222.
[21] J. Sanz-Serna, Markov chain Monte Carlo and numerical differential equations, in: Current Challenges in Stability Issues for Numerical Differential Equations, Springer, 2014, pp. 39–88.
[22] R. Neal, MCMC using Hamiltonian dynamics, Handbook of Markov chain Monte Carlo.
[23] J.-M. Sanz-Serna, M.-P. Calvo, Numerical Hamiltonian problems, Vol. 7, Chapman & Hall London, 1994.
[24] S. Blanes, F. Casas, J. Sanz-Serna, Numerical integrators for the hybrid Monte Carlo method.
[25] A. Beskos, F. Pinski, J. Sanz-Serna, A. Stuart, Hybrid Monte Carlo on Hilbert spaces, Stochastic Processes and their Applications 121 (10).
[26] A. Beskos, N. Pillai, G. Roberts, J.-M. Sanz-Serna, A. Stuart, et al., Optimal tuning of the hybrid Monte Carlo algorithm, Bernoulli 19 (5A) (2013) 1501–1534.
[27] J. S. Liu, Monte Carlo strategies in scientific computing, springer, 2008.
[28] E. N. Lorenz, Predictability: A problem partly solved, in: Proc. Seminar on predictability, Vol. 1, 1996.
[29] E. N. Lorenz, K. A. Emanuel, Optimal sites for supplementary weather observations: Simulation with a small model, Journal of the Atmospheric Sciences 55 (3) (1998) 399–414.
[30] M. Zupanski, I. M. Navon, D. Zupanski, The maximum likelihood ensemble filter as a non-differentiable minimization algorithm, Quarterly Journal of the Royal Meteorological Society 134 (633).

Table 1: RMS error statistics of experiments for assimilation time points $8 \leq t \leq 10$ (after filter stabilizes)

Observation Operator	**Statistics**	**Integrator used with sampling filter**										**Traditional Filters**	
		Verlet		**Two-stage**		**Three-stage**		**Four-stage**		**Integrator on Hilbert space**			
		Fixed step	*Different step*	*Fixed step*	*Different step*	*Fixed step*	*Different step*	*Fixed step*	*Different step*	*Fixed step*	*Different step*	**EnKF**	**MLEF**
Linear observation operator	Min	0.20266	0.192911	0.22185	0.19728	0.218158	0.193404	0.209657	0.194968	1.176385	1.209632	0.153021	0.038487
	Max	0.334077	0.275264	0.371612	0.271278	0.345005	0.27841	0.350564	0.262573	1.740247	2.074682	0.477702	0.122152
	Mean	0.266498	0.2247	0.269914	0.225638	0.263563	0.230312	0.263878	0.227828	1.413573	1.506806	0.305293	0.080486
	Std	0.024486	0.016978	0.026238	0.013978	0.02482	0.017086	0.028621	0.016688	0.097418	0.11711	0.091245	0.021025
	Mean+2*std	0.31547	0.258656	0.32239	0.253594	0.313203	0.264484	0.32112	0.261204	1.608409	1.741026	0.487783	0.122536
	Mean−2*std	0.217526	0.190744	0.217438	0.197682	0.213923	0.19614	0.206636	0.194452	1.218737	1.272586	0.122803	0.038436
Quadratic observation operator	Min	0.293207	0.223915	0.229499	0.227357	0.257983	0.225245	0.26389	0.216563	1.803022	1.873196	3.340558	0.035067
	Max	5.437528	5.710717	3.525457	5.148642	3.286706	5.412255	3.489366	5.042837	3.449921	749.351232	4.555472	0.099079
	Mean	4.492176	2.802898	0.65887	1.161938	0.577684	1.132138	0.645417	0.80452	2.487458	10.76511	3.927612	0.0655
	Std	0.836105	2.326364	0.828443	1.711295	0.662738	1.642162	0.8385	1.295648	0.432504	74.606915	0.323017	0.018352
	Mean+2*std	6.164386	7.455626	2.315756	4.584528	1.90316	4.416462	2.322417	3.395816	3.352466	159.97894	4.573646	0.102204
	Mean−2*std	2.819966	-1.84983	-0.998016	-2.260652	-0.747792	-2.152186	-1.031583	-1.786776	1.62245	-138.44872	3.281578	0.028796
Cubic observation operator	Min	3.005206	0.453015	0.295747	0.475533	0.310439	0.526365	0.293922	0.426434	1.673592	1.684055	5.747101	4.848668
	Max	5.195681	5.083948	3.904205	2.310545	2.606434	2.510949	1.32128	2.505575	2.659555	4659.091624	11.620567	6.695764
	Mean	4.159783	1.514528	1.300494	1.006574	0.606089	1.235655	0.454872	1.071686	2.213129	140.412187	8.768142	5.521612
	Std	0.382443	0.970227	1.153967	0.482539	0.482256	0.519058	0.166534	0.481047	0.220747	607.350568	1.61792	0.48539
	Mean+2*std	4.924669	3.454982	3.608428	1.971652	1.570601	2.273771	0.78794	2.03378	2.654623	1355.113323	12.003982	6.492392
	Mean−2*std	3.394897	-0.425926	-1.00744	0.041496	-0.358423	0.197539	0.121804	0.109592	1.771635	-1074.288949	5.532302	4.550832
Absolute value observation operator	Min	0.223854	0.215914	0.230685	0.215965	0.221819	0.207496	0.213172	0.21736	1.594316	2.086698	0.156432	0.054058
	Max	3.770117	4.278896	4.221607	3.440444	3.783911	3.414783	3.255274	4.605238	3.186142	4.924546	0.489043	0.13553
	Mean	0.390026	0.693854	0.488504	0.591975	0.514439	0.569576	0.401922	0.761355	2.240063	3.662198	0.235906	0.093232
	Std	0.472502	0.938676	0.70202	0.74757	0.719887	0.721405	0.52001	0.993143	0.410658	0.553756	0.101655	0.023183
	Mean+2*std	1.33503	2.571206	1.892544	2.087115	1.954213	2.012386	1.441942	2.747641	3.061379	4.76971	0.439216	0.139598
	Mean−2*std	-0.554978	-1.183498	-0.915536	-0.903165	-0.925335	-0.873234	-0.638098	-1.224931	1.418747	2.554686	0.032596	0.046866
Quadratic observation operator with threshold	Min	0.256795	0.208163	0.25226	0.201484	0.253754	0.207151	0.229083	0.203665	1.348305	1.326491	2.018643	4.562743
	Max	4.585849	4.775978	0.512091	3.665279	0.402913	2.117683	0.415055	0.283818	1.91278	3.690276	3.296156	6.876647
	Mean	3.406461	1.920009	0.303039	0.448207	0.295141	0.290576	0.303422	0.240194	1.579326	1.853404	2.801247	5.539968
	Std	1.067004	1.927817	0.044306	0.686636	0.03201	0.235245	0.037552	0.016292	0.119657	0.456134	0.311357	0.613989
	Mean+2*std	5.540469	5.775643	0.391651	1.821479	0.359161	0.761066	0.378526	0.272778	1.81864	2.765672	3.423961	6.767946
	Mean−2*std	1.272453	-1.935625	0.214427	-0.925065	0.231121	-0.179914	0.228318	0.20761	1.340012	0.941136	2.178533	4.31199
Exponential observation operator with $r = 0.2$	Min	0.318723	0.315953	0.313345	0.296624	0.309291	0.277073	0.321489	0.291672	1.42193	1.408169	2.028516	3.98497
	Max	2.563976	3.075637	0.688663	0.43783	0.643646	0.612475	0.674257	0.439936	1.97735	2.081439	3.911317	5.782877
	Mean	0.433829	0.453889	0.408104	0.348357	0.405423	0.349503	0.408271	0.348964	1.610456	1.661009	3.153979	4.876692
	Std	0.267084	0.320384	0.05718	0.028835	0.055325	0.041517	0.05946	0.02787	0.10526	0.139997	0.551218	0.444681
	Mean+2*std	0.967997	1.094657	0.522464	0.406027	0.516073	0.432537	0.527191	0.404704	1.820976	1.941003	4.256415	5.766054
	Mean−2*std	-0.100339	-0.186879	0.293744	0.290687	0.294773	0.266469	0.289351	0.293224	1.399936	1.381015	2.051543	3.98733

Table 2: RMS error statistics of experiments for assimilation time points $8 \leq t \leq 10$ (after filter stabilizes). The exponential observation operator with factor $r = 0.5$ is used.

Statistics	**Integrator used with sampling filter**	
	Three-stage; $h = 0.01,\ m = 60$	**Hilbert** ; $h = 0.001,\ m = 30$
Min	0.304178	1.234498
Max	2.671971	2.350684
Mean	0.439776	1.699096
Std	0.274643	0.250088
Mean+2*std	0.989062	2.199272
Mean−2*std	-0.109510	1.198920

Table 3: RMS error statistics of experiments for assimilation time points $8 \leq t \leq 10$ (after filter stabilizes). Fixed step size $h = 0.01,\ m = 10$.

Observation Operator	**Statistics**	**Integrator used with sampling filter**					**Traditional Filters**	
		Verlet	**Two-stage**	**Three-stage**	**Four-stage**	**Hilbert**	**EnKF**	**MLEF**
Linear	Mean	0.266498	0.269914	0.263563	0.263878	1.413573	0.305293	0.080486
	Std	0.024486	0.026238	0.02482	0.028621	0.097418	0.091245	0.021025
Quadratic	Mean	4.492176	0.65887	0.577684	0.645417	2.487458	3.927612	0.0655
	Std	0.836105	0.828443	0.662738	0.8385	0.432504	0.323017	0.018352
Cubic	Mean	4.159783	1.300494	0.606089	0.454872	2.213129	8.768142	5.521612
	Std	0.382443	1.153967	0.482256	0.166534	0.220747	1.61792	0.48539
Absolute value	Mean	0.390026	0.488504	0.514439	0.401922	2.240063	0.235906	0.093232
	Std	0.472502	0.70202	0.719887	0.52001	0.410658	0.101655	0.023183
Quadratic with threshold	Mean	3.406461	0.303039	0.295141	0.303422	1.579326	2.801247	5.539968
	Std	1.067004	0.044306	0.03201	0.037552	0.119657	0.311357	0.613989
Exponential with $r = 0.2$	Mean	0.433829	0.408104	0.405423	0.408271	1.610456	3.153979	4.876692
	Std	0.267084	0.05718	0.055325	0.05946	0.10526	0.551218	0.444681

Table 4: RMS error statistics of experiments for assimilation time points $8 \leq t \leq 10$ (after filter stabilizes). The exponential observation operator with factor $r = 0.5$ is used.

Statistics	**Integrator used with sampling filter**	
	Three-stage; $h = 0.01,\ m = 60$	**Hilbert** ; $h = 0.001,\ m = 30$
Mean	0.439776	1.699096
Std	0.274643	0.250088